Portable Multi-Wavelength Fluorosensor Based on UV Light Emitting Diodes

Master's Thesis
by
Sara Ek

Lund Reports on Atomic Physics, LRAP-369
Atomic Physics Division, Lund University
Lund, Sweden

November 2006

Abstract

Optical spectroscopy helps us to understand and observe the physical world. The wavelength specific interaction between light and matter provides information about the chemical constituents of a sample. Fluorescence spectroscopy is one aspect of optical spectroscopy and has many applications. Environmental and medical are of special interest for mankind. In fluorescence the bandwidth of the excitation source is not critical and Light Emitting Diodes (LEDs) could therefore replace the expensive lasers in present fluorosensors. The comparatively low price makes the technology attractive for use in developing countries.

After a thorough investigation of the optimal design, development of system components (optics, fibres, mechanics and electronics) and software algorithms, a portable multi-wavelength fluorosensor based on UV LEDs was constructed. The system is fully computer controlled and self sufficient of power, making it suitable for field use. The fluorosensor shows good performance and was able to diagnose basal cell carcinoma during a photodynamic therapy session.

Contents

Chapter 1

Introduction

1.1 Background

Colour is all around us. It is a sensation that adds excitement and emotions to our lives. Everything from the clothes we wear to the pictures we paint revolves around colour. Colours are often used to describe emotions: we can be red hot, feeling blue or be green with envy. From a medical point of view colour sometimes help us to make a diagnosis. A skin area can be suspected for a malignant lesion because of its reddish appearance. But how can we be sure that what one person calls *red* is the same colour that another person calls *red*? By letting technical equipment measure the intensity at every wavelength instead of relying on the impression of our own eyes it is possible to see well-defined "colours" even beyond the visible area.

Fluorescence is the phenomenon in which absorption of light with a given wavelength by a fluorescent molecule is followed by the emission of light at longer wavelengths. Fluorescence detection has three major advantages over many other investigational methods: high sensitivity, high speed and safety. The point of safety refers to the fact that it is a non invasive method that does not interfere with the sample. The fluorescence signal is proportional to the concentration of the substance being investigated. A small change in concentration will immediately be noted as a change in intensity of the fluorescence peak.

Fluorescence spectroscopy can be used as a diagnostic tool for different malignant diseases; an application that researchers at the Division of Atomic Physics, Lund have been pursuing for more than 20 years. Several fluorosensors using lasers as light sources have been constructed and they are now used at the Lund University Hospital in diagnostic applications.

The task of the present Master's thesis is to develop a technique, based on cheap components, that shows similar performance as a system based on lasers [1]. Because the excitation light levels required to generate a fluorescence signal are low, Light Emitting Diodes (LEDs) should emit sufficient intensity for the task and could therefore replace the expensive lasers. Lasers are often to prefer in optical systems because of their well-defined wavelengths, but this aspect

is not critical in laser-induced fluorescence. The recent progress in the LED manufacturing leading to LEDs in the ultra violet (UV) region to be available on the market was a prerequisite for this project to emerge.

1.2 Goal

The goal with this Master's thesis is to design and develop a device, based on LEDs, that detects the fluorescence from a sample. It should be able to emit several different excitation wavelengths which are easily altered via the computer software. To make it suitable for field use the system should be made as small as possible making it easy to transport, and be self sufficient of power.

The system developed is expected to have many applications in environmental and medical contexts. The fact that it is comparatively low price and robust also makes it attractive for use in developing countries, an aspect which has been emphasized in earlier spectroscopic contexts [3, 2].

1.3 Scope of thesis

The thesis work includes thorough investigation of the optimal design, development of system components (optics, fibres, mechanics and electronics) and development of software algorithms that control the system.

Some final fluorescence measurements are performed to demonstrate the system performance.

1.4 Outline

First the reader is introduced to the subject by a brief theory chapter, Chap. 2, describing the basic principles of a LED and the phenomenon of fluorescence. To get a feeling of the information the spectral signature can provide a few applications are described in chapter 3. The possibility to measure the accumulation of AGE-products (Accumulation of Advanced Glycation End products) is a novel and interesting application. In chapter 4 the reader is invited to follow the design discussion prior the final construction which is followed by a documentation of equipment,Chap. 5. The results from measurements are presented and discussed in chapter 6. The thesis ends with summary and conclusions, Chap. 7 and desirable future improvements, Chap. 8. A construction kit with budget and drawings can be found in Appendix A.

Chapter 2

Theory

2.1 Light-emitting diodes

A light-emitting diode (LED) is a semiconductor device that emits incoherent light when biased in the forward direction. The colour of the light emitted depends on the chemical composition of the semiconducting material used, and can be near-ultraviolet, visible or infrared. The first LEDs were made of gallium arsenide and emitted red or infrared light. Advances in materials science have made it possible to manufacture devices with shorter wavelengths all the way down to 250 nm. The UV LED are more difficult to manufacture, also because the UV light causes photodegradation to the clear epoxy case that encloses the semi-conductor chip in the LED [4].

The chip consists of two doped semiconductor regions separated by a junction. One of the two regions is dominated by positive electric charges (p-type), the other is dominated by negative electric charges (n-type). When sufficient voltage is applied over the chip the potential barrier is reduced and electrons in the conduction band are able to recombine with the holes in the valence band; see Figure 2.1. The excess energy created in the recombination can be emitted in the form of a photon. Only photons in a limited frequency range can be emitted by any material, because the photon energy depends on the energy band gap of the semiconductor material [5, 6].

A light-emitting diode should not be confused with a diode laser that emits coherent narrow-band light. In the diode laser the active crystal is cleaved to get perfectly smooth, parallel edges, forming an optical cavity. Photons emitted into a mode of the waveguide are reflected several times and the light is amplified by stimulated emission. The amount of light is reduced by absorption and incomplete reflection at the end facets. When amplification is greater than losses the diode begins to lase. Before that it acts as a LED [7].

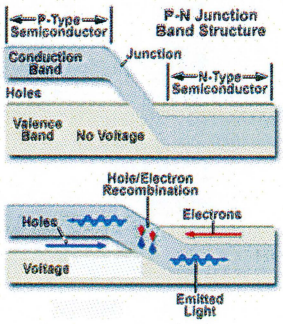

Figure 2.1: pn-junction. (From [6]).

2.2 Fluorescence

A molecule possesses different energy levels according to the rules of quantum mechanics. If an incoming photon has an energy that corresponds to the gap between two energy levels in the molecule, it can get absorbed. The de-excitation of the molecule can follow several different pathways as indicated in Figure 2.2. Emission of fluorescence light is one of the possible processes. The energy levels can be shown in a so called Jablonski diagram, where $S_0, S_1..$ are singlet electronic states. In a singlet excited state the electrons are said to be paired, they have opposite spin orientation. In the triplet states $T_0, T_1..$ their spin have the same orientations [8, 9].

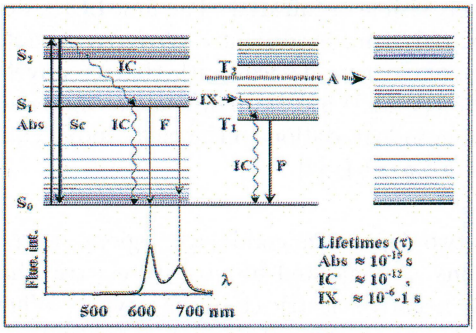

Figure 2.2: Jablonski diagram. (From [10]).

The absorption process is instantaneous and thus the atoms do not move during the process (Franck-Condon principle). This has as a consequence that the molecule is not necessarily excited to the lowest vibrational level but more likely to a higher state. Due to the high density of vibrational and rotational states a rapid relaxation to the S_1 state takes place. From the lowest vibrational state the molecule is quantum mechanically allowed to return to the S_0 state. The excess energy, corresponding to the molecule band gap, is emitted in the form of a photon. The process is called fluorescence. As seen in Figure 2.2, transitions between states with different multiplicity are possible, i.e. a triplet excited state can combine with a singlet ground state. Such transitions have a low probability and thus the emissive rates are slow. The phenomenon is called

phosphorescence. Phosphorescence is often week in room temperature, but is enhanced at low temperatures when competing processes are reduced [10].

Chapter 3

Applications

3.1 Accumulation of Advanced Glycation End (AGE) products measured as skin autofluorescence

AGEs (Advanced Glycation End) products are produced when sugar and lipids react with proteins. AGEs can accumulate in nearly every type of cells in the body. It is thought to be the major factor in aging and age-related chronic diseases, such as diabetes, Alzheimer's disease, atherosclerosis and chronic renal failure. AGE is the result of a chain of chemical reactions after an initial glycation reaction. Glycation is when a sugar molecule bonds to a protein without the controlling action of an enzyme. The accumulation of AGE-related damage is therefore proportional to the intake of unhealthy food containing glycation forming sugars such as fructose and glycose. Many cells in the body bear the receptor for AGE and the accumulation affects the structure and function of the proteins [11, 12].

Since the skin is constantly exposed to harsh environmental conditions such as UV radiation, wind, cold, heat and pollutants, it requires a mechanism of repair. It is expected that the ability of the skin to repair itself reduces with age, but also the accumulation of AGE is a contributing factor in the aging of proteins [13]. Even though a plastic surgeon can do a remarkable job the skin will still have a aged appearance when studying the fluorescence spectra. Stamatas *et al.* have shown that the intensity of skin autofluorescence is age dependent, see Figure 3.1.

AGE accumulation increases during renal failure, because then the kidney effectiveness of removal of AGE is reduced, and during diabetes, because of the increased blood sugar levels. If the accumulation could be measured it would provide a tool for assessing the risk of long-term complications. Several AGE components fluoresce at 440 nm when illuminated with 370 nm, why a fluorosensor in the UV region, like the one developed in this project, could be useful for the measurements.

Meerwaldt *et al.* have developed an autofluorescence reader using an excitation

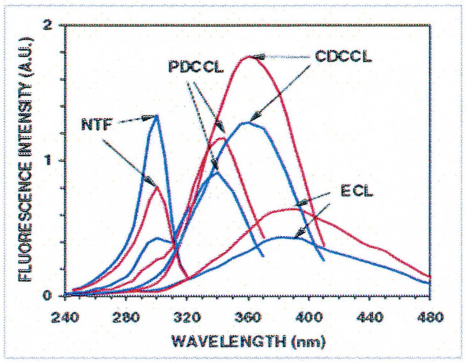

Figure 3.1: Typical excitation spectra taken on the cheek area of two individuals, aged 30 and 60 years, blue and red lines, respectively. The fluorescence band of epidermal tryptophan moieties (NTF) decreases with age, whereas dermal fluorescence from collagen and elastin cross-links (CDCCL, PDCCL, ECL) increase (From [13]).

light source between 300 and 420 nm for the non-invasive measurements of the skin autofluorescence [14]. The measurements with the autofluorescence reader were made in a semi-dark environment. In order to suppress stray light and only detect the skin autofluorescence, control measurements were made in a dark environment. The fibre probe was placed on a nonpigmented skin with limited sun exposure on the lower part of the arm. Skin pigmentation may absorb light and influence the autofluorescence. By comparing the reflectance on the skin and on a white Teflon block (assuming 100% reflectance) the problem could be avoided. Figure 3.2 shows the result when measuring the difference in skin autofluorescence between a Type 1 diabetic patient and a control person.

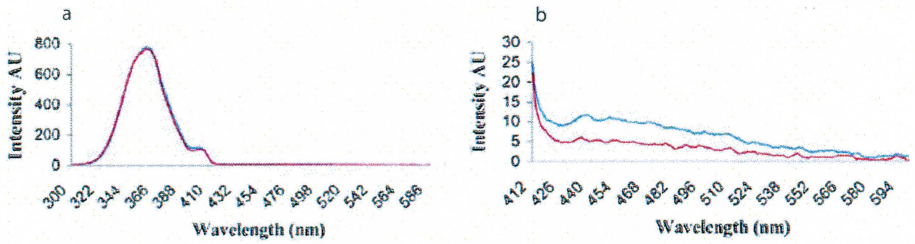

Figure 3.2: a. Emission spectrum (420-600 nm) for a Type 1 diabetic patient (blue line) and a matched control subject (red line). b. Analyzed data showing the difference in intensity between a Type 1 diabetic patient (blue line) and a matched control subject (red line) (From [14]).

One should always have in mind how much the skin-autofluorescence can reveal about the patient medical state. There may be valuable hidden variables in the results from other spectroscopic investigations, like cancer diagnostics.

3.2 Diagnosis and treatment of superficial cancer

As long as cancer plagues humanity researchers worldwide will continue to find new methods to fight the malignant cells. A definite diagnose usually requires a histological examination of the tissue. The tissue sample is obtained by biopsy or surgery. Once diagnosed, cancer is usually treated by a combination of surgery, chemotherapy and radiotherapy. There are hundreds of different types of cancer and treatments are becoming more specific for the type of cancer pathology. The methods of treatment mentioned above may themselves induce malignancy or the patient may be physically impaired for a longer period of time. In this section the possibilities to use light for both detection and treatment of tumours are discussed.

3.2.1 Using autofluorescence to differentiate basal cell carcinoma from normal skin

Fluorescence detection helps demarcate skin cancer from normal skin. Basal Cell Cancer (BCC) constitutes the most common type of skin malignancy world wide, nearly 2 million new cases are diagnosed annually. BCCs are slow-growing, locally invasive tumours that rarely metastasize but can be destructive and disfiguring.

Today the standard procedure to diagnose skin cancer is to take a biopsy which is histologically evaluated. To be able to do a biopsy the lesion needs to be visible. In order to detect the cancerous tissue in an early state and accurately define the affected area, a non-invasive screening technique is desirable. The light interaction with tissue provides information about the chemical composition of the tissue.

When the skin is illuminated the autofluorescence spectrum ranges from blue to red. Both the BCC lesion and the surrounding skin have an intensity maximum at 455 $\pm$ 3nm. Wulf *et al.* [15] found that the peak intensity on the average was 53% lower in the tumours than in normal skin, see Figure 3.3. However other groups using the excitation wavelength 375 nm, have not found any difference in the total fluorescence, but they did not compare the peak intensities. Brancaleon *et al.* used 295 nm excitation and noted that the fluorescence from the tumour was much stronger than that of the surrounding healthy tissue. The reason is thought to be due to the hyperactivity in the tumour creating tryptophan moieties. When using the excitation wavelength 410 nm, which is strongly absorbed in hemoglobin, the intensity difference may be related to increased blood supply in tumours. It is obvious that the wavelength plays an important role in the effectiveness of using fluorescence for skin cancer diagnosis, why an instrument with several different excitation wavelengths would be of interest [16].

There is a great advantage using autofluorescence in cancer demarcation, since there is no need of introducing sensitizing drugs on the tissue. The investigations that have been made suggest that autofluorescence-based image processing of BCC may be possible, which would fulfill the wishes for a fast, non-invasive screening technique. Further knowledge about the mechanisms that

cause changes in the cancer autofluorescence is needed and investigations made show that it is worthwhile [15].

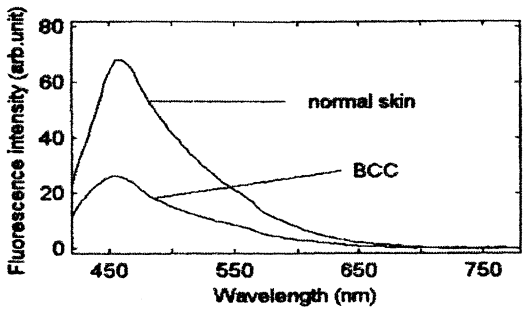

Figure 3.3: Typical autofluorescence spectra recorded from basal cell cancer and normal skin. The excitation wavelength was 370 nm (From [15]).

With a photosensitizer and tissue oxygen is present it is also possible to treat tumours with light.

3.2.2 Photodynamic therapy

Photodynamic therapy, or PDT, has been performed since the 1960's. It is a treatment that enables selective termination of cancer cells. The technique requires three components: therapeutic light, a photosensitizer and tissue oxygen. PDT is limited by the penetration depth of the light. Development of sensitizers active in the near-infrared region has increased the penetration to about 4-6 mm. Inserting multiple optical fibres into a larger tumour mass makes it possible to treat thick tumours and tumours embedded in healthy tissue [17].

When treating skin cancer a photosensitizer cream can be applied onto the diseased area. The sensitizer protoporphyrin IX (PpIX) precursor δ-amino levulinic acid (ALA) is a natural constituent in the body, utilized as the starting material in the haem cycle. PpIX is produced at higher concentrations in diseased cells than in healthy areas. After allowing the sensitizer to build up for a few hours the tumour and part of the surrounding healthy tissue is illuminated with therapeutic light. Since the technique is selective, healthy tissue are illuminated at low risk. It is important to treat the entire tumour, even the cancer tissue that is not visible for the naked eye, otherwise there is a risk for recurrence. The wavelength of the light matches the absorption of the sensitizer and light will get absorbed in the tumour. The absorbed energy may be transferred from the metastable triplet state of the sensitizer to a neighboring oxygen molecule, forming singlet oxygen $[O_2(^1\Delta_g)]$. Singlet oxygen is highly oxidative and will almost immediately react with its closest surrounding (within an estimated radius of 0.01-0.02 μm). Since the sensitizer, and therefore also the singlet oxygen is mainly located in the tumour it will react with malignant cells - causing a primary tissue necrosis [18].

Figure 3.4 is a schematic view of PDT using PpIX (Protoporphyrin IX) as a sensitizer. The sensitizer acts as a catalyst. After the energy transfer it returns

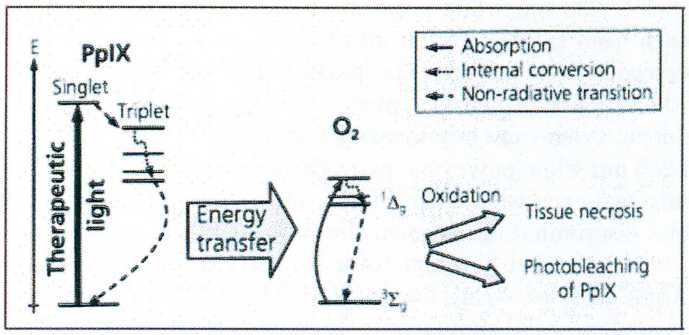

Figure 3.4: The principle of PDT (From [18]).

to its original state and can be activated again. However, the singlet oxygen produced may oxidize the sensitizer instead of a malignant cell making the PDT process self-terminating. This process is called photobleaching and prevents the lesion from getting over-treated [18].

PpIX has a series of absorption bands, ranging from the Soret band at 400 nm to a weak band in the red region centered around 635 nm. Thus a light source that peaks around 630-635 nm is optimal. Lasers are normally used since the light has a well defined wavelength and is easily guided through an optical fibre. Recently, however, it has become possible to produce light sources consisting of arrays of LEDs, which are selected to closely match the 635 absorption profile of PpIX [19]. Such a LED array is now used at the Oncology clinic at the Lund University Hospital as a complement to laser-based systems.

3.3 Detection of aromatics in oil polluted soil and water samples

Laser induced fluorescence (LIF) spectroscopy has drawn considerable interest in remote sensing of various pollutants in air, water and soil. At the Atomic Physics Division at the Lund Institute of Technology a mobile LIDAR (Light Detection And Ranging) system has been employed. The system has measured the sulphur dioxide concentration in the smoke and ash plume from Mount Etna on Sicily, Italy, monitored the facades of historical-buildings like the Coliseum in Rome and has studied marine oil spill pollution. In a similar, down scaled manner aromatic hydrocarbons in oil contaminated water and soil samples can be detected with a small, portable fluorosensor.

The optical density of an oil layer increases dramatically below 350 nm. The fluorescence intensity increases by reducing the excitation light wavelength. Petroleum products (e.g. diesel fuel) are complicated mixtures of mono- and polycyclic aromatic hydrocarbons (PAHs) and the fluorescence changes the intensity and the decay characteristics significantly when illuminated with different excitation wavelengths. Diesel fuel consists in average of paraffins, naphthenes, aromatics, and additives. Paraffins and naphthenes have only strong

absorptions below 230 nm while aromatic hydrocarbons show strong absorptions that reach from the UV region into the visible spectrum. UV excitation induces fluorescence from the aromatic parts in the oil. The absorption region depends on the number of benzene rings. Monocyclic aromatic hydrocarbons (benzene, toluene, xylene and ethylbenzene) only absorb light with wavelengths shorter than 280 nm while polycyclic hydrocarbons also have absorptions above 300 nm. Using two excitation wavelengths, one below 280 nm and one above 300 nm enables discrimination between the two. J. Bublitz *et al.* have used the combination 355 nm (third harmonic of a Nd:YAG laser) and 246 nm (stimulated third Antistokes scattering line in H_2). The different classes of aromatic hydrocarbons are better discriminated if time-resolved LIF detection is possible. The detection limits when using lasers with typical pulse powers of 2 μJ/pulse is 0.5 mg engine oil/L in water and 5 mg engine oil/kg in soil with the Bublitz *et al.* setup [20]. The detection limit would probably be significantly higher when using LEDs because of the loss in coupling efficiency.

Chapter 4

Construction of the fluorosensor

By analyzing the fluorescence signal from a sample it is possible to determine the existence and concentration of the investigated molecule. The experiment setup is quite simple. The sample is illuminated with light with a wavelength that the fluorescent molecule is able to absorb. After the molecule has incorporated the photon a part of the absorbed energy is transferred, due to internal conversion, and the molecule then emits light with a longer wavelength. To avoid saturation of the detector it is important to filter out the reflected light, which can be done with coloured-glass filters, see Figure 4.1.

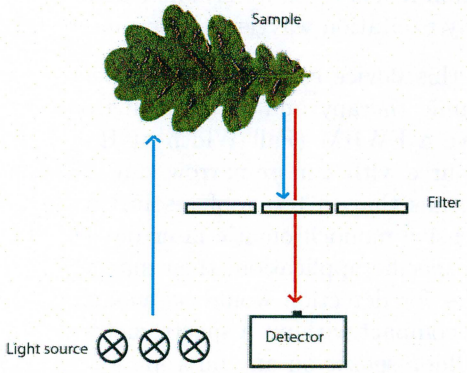

Figure 4.1: The experiment setup. The sample is illuminated with UV light and the red-shifted fluorescence light is detected. The reflected UV light is filtered out with coloured glass filters.

By illuminating the sample with several different wavelengths the fluorescence signals will give more information about the sample. When using several different excitation wavelengths it is important not to filter out the fluorescence peaks close to the excitation wavelength. It is mostly in that area the fluorescence signals differ between the different cases. Further out towards the red the signals from the different cases may look very similar to each other. In Fig-

ure 4.2 some Italian marble samples have been illuminated with four different wavelengths, and the figure clearly show that the spectra vary depending on sample and excitation wavelength.

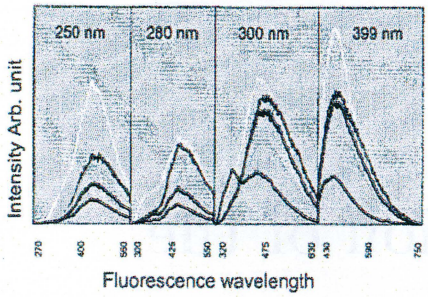

Figure 4.2: Four different marble samples (the different coloured spectra in each figure) have been illuminated with four different wavelengths (the four different figures). By using a filter with a cut-off as close to the excitation peak as possible it is easier to separate the different samples (From [21]).

4.1 Design considerations

There are many different possibilities how to construct this fluorosensor. Many different aspects must be taken into account in order to create a portable, cheap fluorosensor capable to record signals with a sufficient signal-to-noise ratio. Depending on application it has to be determined what system resolution is necessary and how many excitation wavelengths are interesting.

It is desirable that this device can accumulate spectra like fluorescence from PpIX in photodynamic therapy and chlorophyll from vegetation. These fluorescence peaks have a FWHM (Full Width at Half Maximum) of about 20 nm; hence a light source with a more narrow emission profile than that would be overkill. This means that in terms of resolution cheap LEDs can be used just as well as expensive monochromatic laser diodes. If the fluorosensor was constructed for one specific application, then maybe a design with four LEDs and four photodiodes for detection would be enough. In that case the device could be made very compact without a spectrometer. It is, however, desired to be able to use this fluorosensor on any fluorophore that absorbs UV, or other wavelengths, since the LEDs and filters are replaceable. A spectrometer with an array of diodes is therefore required. Which wavelengths to be used for excitation also need to be considered. If the device would be constructed for medical applications regarding ALA photo dynamic therapy only, then maybe one LED at 405 nm would be enough. The design could consist of one fibre coupled to the LED leading the light to the sample, and another fibre collecting the fluorescence and direct it through an Inline Filter System, see Figure 8.4 before reaching the spectrometer. However a multi-wavelength system will always provide more information in every application. If as many as eight wavelengths were to be used, they either have to be placed on a multi LED chip; see sec-

tion 2.1, or on a rotating/sliding arrangement, but this would require a larger box. But maybe the fluorosensor can consist of half as many LEDs without any information being lost. To illustrate this cases Figure 4.3 presents excitation spectra for PpIX fluorescence at λ_{em}= 705 nm. The peak around 400 nm is about 40 nm in FWHM and if several LEDs around 395-405 nm are used they would probably give very similar result.

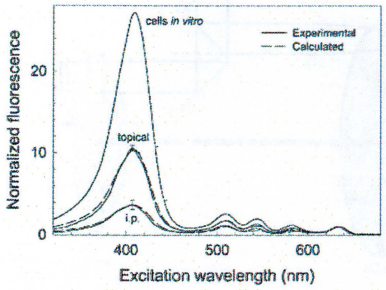

Figure 4.3: Excitation spectrum of PpIX fluorescence at λ_{em}= 705 nm. The spectra are normalized to 1 at λ=633 nm (From [22]).

In the following design discussion three or four LEDs in the wavelength region 250-400 nm are thought to be included.

4.1.1 Sliding vs. rotating arrangement

The first idea was to design the fluorosensor as shown in Figure 4.4a. The LEDs and the filters are placed on the same axis which is movable back and forth. This solution could be difficult to fit into a small box, why the idea to adjust the sliding arrangement as shown in Figure 4.4b came to mind. These solutions

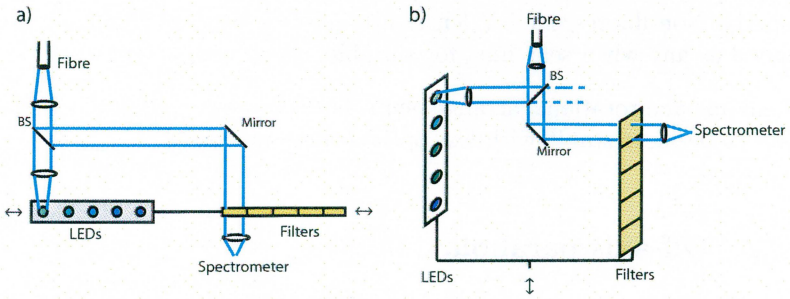

Figure 4.4: Sliding arrangement

would have given poor stability. It is important to make a robust construction because the slightest movement will cause great loss in light intensity. It was also difficult to figure out how to control this sliding arrangement automatically. The axis with the LEDs and filters attached could be placed on a sledge steered by a cogwheel.

It seemed easier to apply an automatic control of the system if the movement is rotational instead of sliding, see Figure 4.5. This would also make the system more stable and compact, allowing a smaller box for the final result. In the

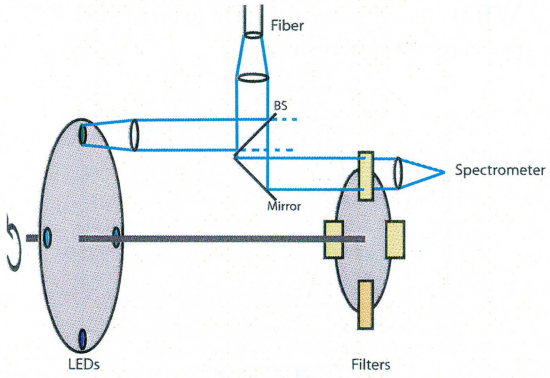

Figure 4.5: Rotating arrangement

three setups discussed so far a beam splitter and several lenses are used. When the light from the LED first hits the beam splitter 50 % of the light is focused into the fibre probe, the rest is lost. After interaction with the sample only 50 % of the returning light will be focused towards the detector. This sums up to 75% loss between the LED and detector. In addition to these evident losses in the beam splitter there will be additional losses in the coupling into the fibre and the spectrometer slit. Because there is no need for a spliced fibre a thick fibre (600 μm to 1 mm) could be used and improve the coupling into the fibre.

It is desirable to insert as few optical components as possible in the light path because at every surface there will be a 4% loss, due to the Fresnel law. When handling as short wavelengths as in this project, down to 250 nm, chromatism in the lenses is also an issue. The refractive index of the material in the lens changes substantially in the UV region and will therefore not focus the UV light properly. Non-fluorescent UV lenses are quite expensive, which is an argument as good as any when searching for suitable, cheap components.

The sliding and rotational arrangements discussed were not optimal. The system needs to be more stable with less optical components.

4.1.2 Off-axis parabola

The polar diagrams over the emission profile from the commercially available UV LEDs with ball lens looked surprisingly parallel and not as divergent as predicted. If that is the case then maybe an off-axis parabola could be a part of the perfect solution. An off-axis parabola can only focus parallel light to a point or the other way around, not from a point to another point like biconvex or planar convex lenses can. The mirror needs to have an optical coating for protection and reflectivity enhancement. Aluminium with magnesium fluoride coating (Al/MgF_2) is superior in UV applications; the aluminium because of

its reflectance and the magnesium fluoride because it retards the oxidation and provides some abrasion protection [23].

The most promising design of the fluorosensor using an off-axis parabola is presented in Figure 4.6. By using a small off-axis parabola and a large lens the

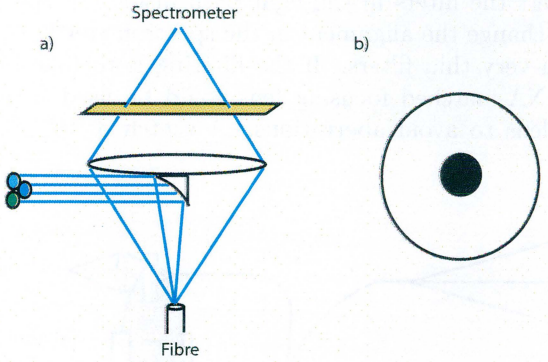

Figure 4.6: a) The light from the three LEDs is focused into the fibre via an half inch sized off-axis parabola. The returning light is focused in a large lens onto the spectrometer slit. b) A figure over the lens and the small part in the middle shadowed by the parabolic reflector.

loss of light will in theory be considerably less than when using a beam splitter. If the parabolic mirror is half an inch in diameter and the lens is two inches, the parabola will only shadow 6,25% of the lens, that is to be compared with the 75% loss using beam splitter. The filters still need to be shifted depending on the excitation wavelength. They should preferably be placed in front of the lens to avoid chromatism, but on the other hand it is desirable to place the parabola as close to the lens as possible, maybe even glued on to the lens surface. Where to place the filter is easiest tested experimentally.

It is very difficult to focus the light with an off-axis parabola, and the fact that the light is not perfectly parallel but quite divergent aggravates the task further. It is easiest to collect the light close to the LED, where the emission profile is still quite narrow. This is where the idea to use all fibre optics was born.

4.1.3 All fibre optics

In a design using all fibre optics the idea was to place a fibre end facing the LED, hoping to collect as much light as possible. This would eliminate lenses and beam splitters and issues like chromatism and intensity loss would be reduced. There will, however, still be other problems in the system. One potential problem is that the autofluorescence in the fibre can cause a high background signal in the measurements. There can also be great losses in the coupling of light into the fibre. Since it is difficult to find the optimal position for the fibre, the LEDs and the fibre ends need to be stationary positioned and a wheel of rotating LEDs is probably not an option. Because of this it is necessary to have a split fibre with three fibres coupled into one. Experimental work has to show which is the most photon economical, loosing light in the split fibre or loosing photons in the coupling between one fibre end and rotating diodes.

The probe facing the sample also needs to be a split fibre. With one fibre guiding the light from the LED and one guiding the fluorescence light to the spectrometer. Unfortunately, the detection fibre cannot be coupled directly into the spectrometer because the light first needs to be filtered. It is desirable to be able to filter the light without disturbing the fibre optics. The only way would be to insert the filters in the light path inside the spectrometer. That would probably change the alignment in the spectrometer but it could perhaps be possible with very thin filters. If the filtering is to take place outside the spectrometer a NA-matched focusing lens could be used with a filter placed in front of the lens to avoid aberrations. A sketch of the setup is shown in Figure 4.7.

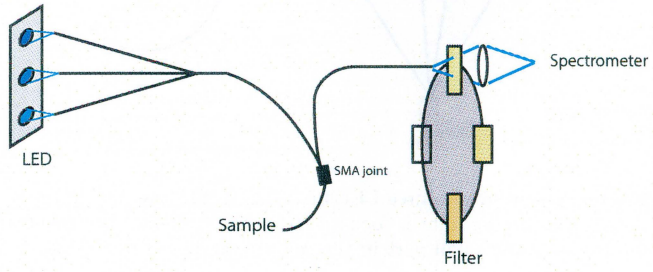

Figure 4.7: Fibre arrangement

4.2 Final design

The discussion above resulted in a fibre-optic design with rotating filters in front of the spectrometer, as shown in Figure 4.7. To avoid using a larger box than absolutely necessary, the optics need to be aligned before insertion. Mounting all the optics on a plate will also make the construction more stable. Figure 4.8 shows two three-dimensional views of the construction. To save space and money the fibres are placed on brackets and not in translating mounts. The brackets can be adjusted the in x- and z- directions and the LEDs which are attached to the vertical part of the mounting plate can be adjusted up and down in the y-direction. The alignment calls for a lot of patience but the brackets turned out to do the job just as well as professional mounts. The LEDs are soldered on to three separate cards and they can easily be replaced. It is very important to make a construction that enables adjustments in every direction. The entrance aperture into the spectrometer is only 200 μm wide and needs to be exactly positioned in the lens focal point. In this design the spectrometer can be adjusted back and forth in the z-direction and the lens is placed in an x- and y-translating mount, making it possible to find the optimal position. To avoid any pressure and damage to the spectrometer it was encapsuled in a mount made of nylon perfectly matched to the spectrometer thickness. The spectrometer position is fixated with one metallic plate on each side. A servo bracket was designed to mount a servo arrangement with the filters attached and the fibre tip facing the spectrometer. The box chosen (from ELFA) is made of thick polystyrol and has mounts for nuts to fasten the baseplate in the bottom.

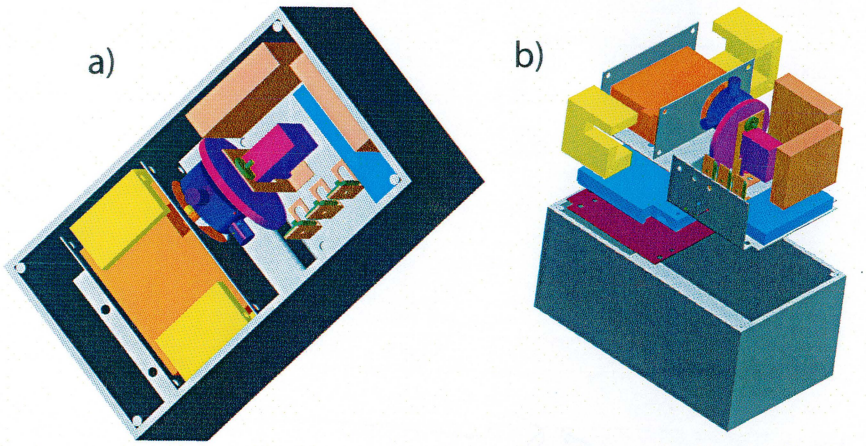

Figure 4.8: The final design. a) Every item on its correct position in the box. b) The box in an extracted view

All the different items are numbered and named in Figure 4.9.

To visualize the final fluorosensor and create proper drawings the project was designed in ProEngineer. The drawings and materials needed are found in Appendix A.

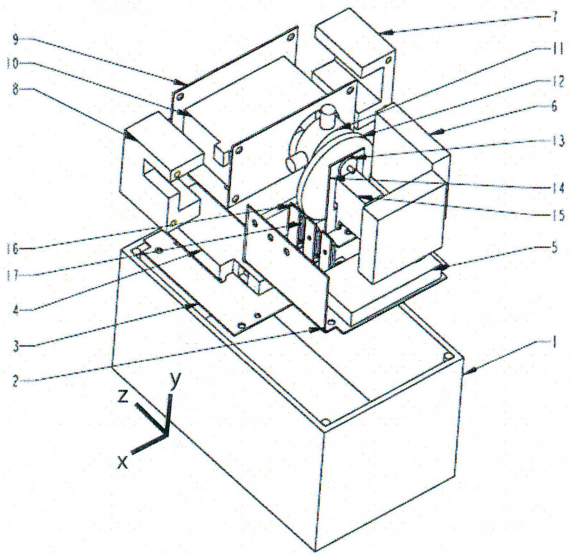

Figure 4.9: 1) Box 2) Baseplate 3) Mounting plate for Data Acquisition card 4) Data acquisition card 5) Printed circuit board controlling the LEDs 6) Battery 7) Spectrometer holder 1 8) Spectrometer holder 2. 9) Plate for spectrometer mount 10) Spectrometer 11) Translating lens mount 12) Filter plate 13) SMA fibre adaptor 14) Servo bracket 15) Servo 16) Fibre mounting bracket facing LED 17) SMA fibre adaptor

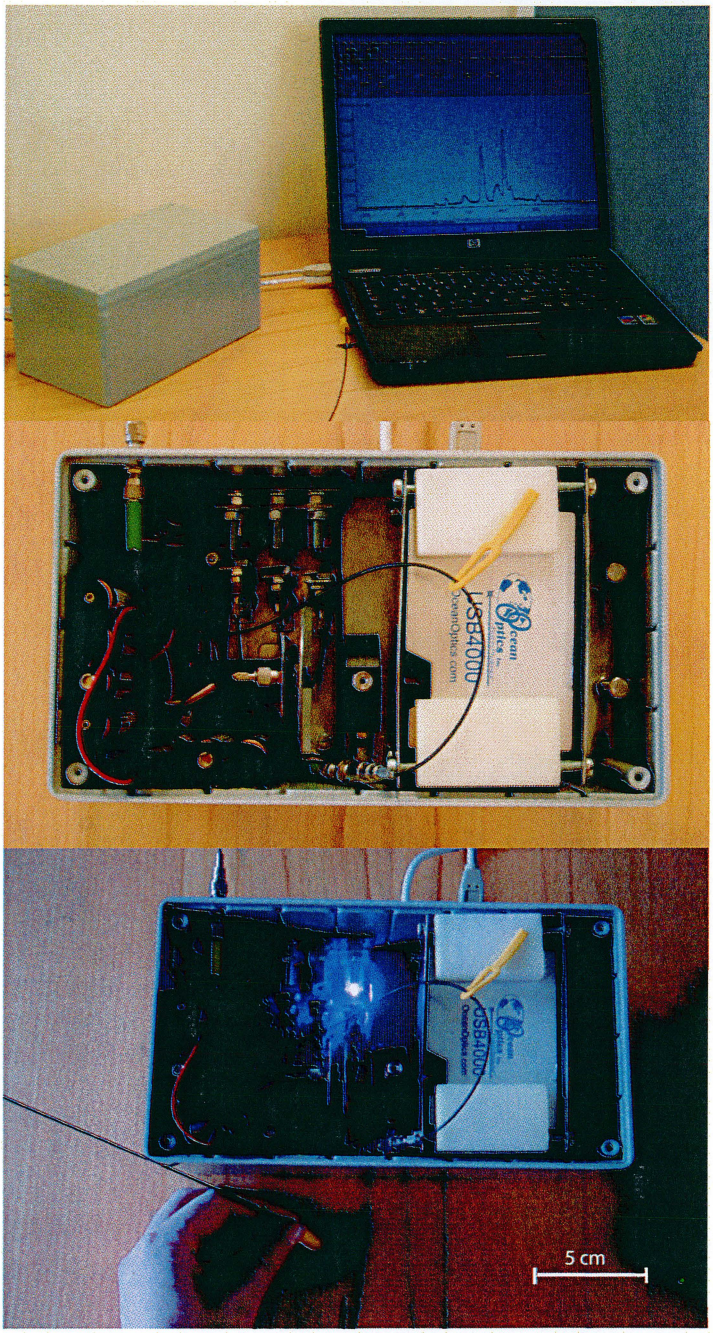

Figure 4.10: Photographs of the constructed fluorosensor.

Chapter 5

Equipment

5.1 Light emitting diodes

In the magazine Laser Focus World it was in May 2006 reported on a multichip deep-UV LED. SETI (Senior Electronic Technology; Columbia, SC) has created the multichip device with eight or more LEDs of different wavelengths [24]. The idea is to produce a broadband UV source, but if each LED can be switched on separately it would be very interesting for this project. This technology is new and is not commercially available yet.

Since the UV LED is a relatively new product on the market the selection is limited. Roithner Lasertechnik, Austria, was found to have the best selection of UV LEDs. A AlGaN/GaN LED chip is encapsulated in a metal-glass package with UV-transparent optical window. The forward current is 20 mA and a typical forward voltage of 6.5 V. Figure 5.1 show the emission profile and measured FWHM (Full Width at Half Maximum) for the LEDs chosen in the final design. The profiles are very broad in comparison with monochromatic lasers, but that will not affect the systems resolution. Typical spectra from laser induced fluorescence were studied and the spectral signature from chlorophyll has a FWHM of 25 nm and PpIX about 20 nm, and will not be much influenced by the LED profile. The intensity on the other hand might be slightly affected by the LED tail towards the visible if not compensated correctly. In Figure 5.2 all three emission profiles, filters and fluorescence spectra from chlorophyll and PpIX are illustrated together, to get a feeling of the magnitudes. All spectra are normalized and the filters are approximate.

Unfortunately there was no power meter for wavelengths below 400 nm available in the laboratory and the output power could not be measured. The supplier did not have that information about the LEDs either, but it should be around 7 mW. To get an idea of how much light that was coupled into the fibre a relative power measurement was performed using a photodiode, see section 8.1. Time acquisition of the LED emission profiles showed that they emit stable light with maximum output power after about 0.3 s.

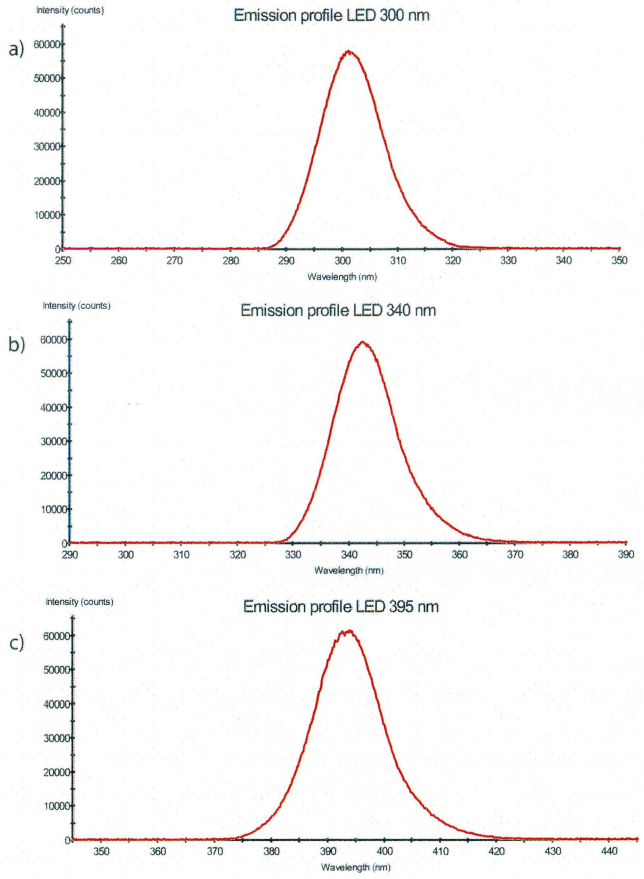

Figure 5.1: Emission profiles for the LEDs used in the fluorosensor. a) LED 300 nm. Max: 300 nm FWHM: 13.8 nm b) LED 340 nm. Max: 342 nm FWHM: 13 nm c) LED 395 nm. Max: 390 nm FWHM: 18.7 nm

5.2 Lens

In the final design the light is filtered just before entering the spectrometer slit. In order to detect sufficiently much light a focusing lens behind the filter is necessary. It is important to choose a lens with good transmission characteristics for ultraviolet wavelength. For this project a UV Grade Fused Silica lens from Edmund Optics was chosen. To optimize the throughput in the ultraviolet region the lens was anti-reflection coated. The size of the lens needs to be matched with the numerical aperture of the fibre.

The fibre emission angle θ was determined using a screen and a ruler. The fibre was placed 50 mm from the screen and the spot size on the screen measured to 11.4 mm.

$$\tan\theta/2 = \frac{11.4}{50} \Rightarrow \theta = 25.7^\circ$$

The fibre numerical aperture was calculated: $NA = \sin\theta/2 = 0.22$. This value corresponds to the NA value given from the fibre manufacturer. An effective

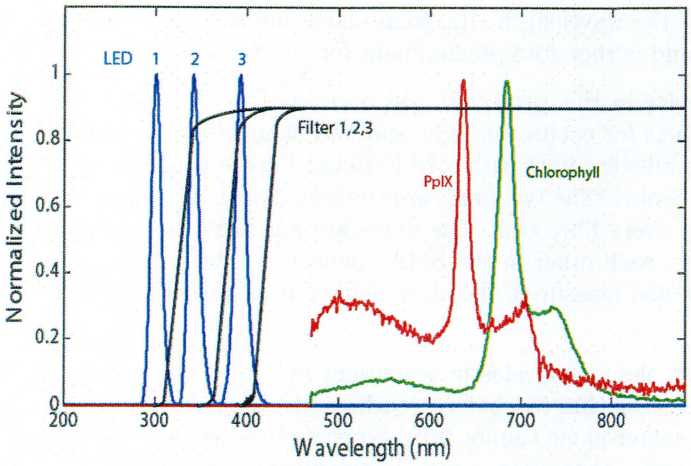

Figure 5.2: All three LED emission profiles and fluorescence spectra from chlorophyll and PpIX. The filter transmission curves are approximate.

focal length, f, of 10-20 mm is desirable why a lens diameter, d, of 4.5-9 mm is suitable, since $d = 2f \cdot \tan\theta/2$. A 9 mm diameter plano-convex lens with effective focal length 13.5 mm was chosen.

The focusing of the fluorescence light into the spectrometer slit is the most critical part of the setup. To enable fine adjustment the lens was placed in a translating lens mount. The curved surface should placed first in the light path. In this way both lens surfaces contribute to changing of the light direction and the aberrations will be smaller.

5.3 Fibre

In order to get sufficient power out of the fibre it is important to use a high-power LED with a correct numerical aperture. If the emission profile is too wide in relation to the acceptance cone of the fibre the coupling efficiency will be reduced [25]. This is difficult to achieve since the emission profile of the LEDs is very wide and would require a very thick fibre. A thick fibre is easily broken and the coupling efficiency into the detector will be bad. The Nonimaging Solar Energy Group at University of Chicago [26] has developed a fibre that concentrates the light and achieve performance thought to be impossible. It has a conical design with a wide core diameter on one side and a smaller on the other. This is very interesting and will hopefully be commercially available soon.

Optical fibres are used in the wavelength window between the absorption region in the UV and another absorption region in the infrared. Absorption in the UV region is due to the fact that the photons carry sufficient energy to excite the electrons of the glass into the conduction band. In the infrared region the absorption is due to molecular vibrations. There are other processes that cause losses in the fibre. In the UV region Rayleigh scattering dominates. Rayleigh scattering is when the light is scattered from small particles with size up to $\lambda/10$

, where λ is the wavelength. Rayleigh scattering is very wavelength dependent, $I \sim 1/\lambda^4$, and is therefore predominant for shorter wavelengths.

For the device in this project it was necessary to use a split fibre probe with three channels for excitation light and two channels for spectroscopy; see Figure 4.7. An all-silica fibre with core 400/clad 440 μm was purchased from A.R.T. Photonics GmbH. The two parts are connected with a SMA joint and has SMA attached to every fibre end. The fibres are not fused together but only placed very close to each other in the SMA connector. The autofluorescence induced in the fibre was measured, but does not seam to have any significant affect on the result.

To suppress the strong elastic scattering by the exciting light the incoming light needs to be filtered before reaching the spectrometer. This is because the spectrometer alone cannot fully suppress this intense light which can cause saturation and a phenomenon called "blooming" in the detector; see the section 5.5.

5.4 Filter

When the excitation light reaches the sample not all photons interact with the material. Many of the photons are reflected. The reflected light, that has the same wavelength as the excitation light, has a much higher intensity than the shifted fluorescence light. To be able to detect the fluorescence signal it is necessary to suppress the reflected light. This can be done using optical glass filters which act as long-pass filters that block short wavelengths. Figure 5.3 shows a transmission curve for Schott optical glass GG385. The transmission curves for GG420 and WG280 that are also used in the setup look similar except for the different cut-off wavelengths at 420 nm and 280 nm respectively.

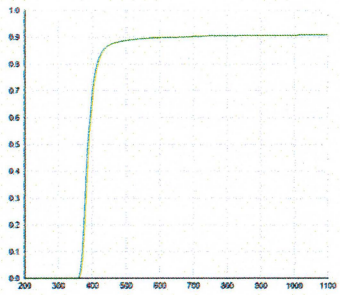

Figure 5.3: Transmission curve for coloured glass filter 385 nm (From [27]).

Even though the transmission curve looks nice and steep and the material normally has low self-fluorescence, there may be problems in our applications. The reflected light to be filtered out has a very strong intensity in the UV which can induce fluorescence in the material which is not negligible when detecting week signals.

In this project LEDs are used as light sources and not monochromatic lasers. This can cause problems because the emission profile is about 12 nm wide and

there is a weak tail towards longer wavelengths, where the fluorescence occurs. In the LED datasheet the FWHM (Full Width at Half Maximum) is defined but it is a big difference if the emission profile is steep or flat with a long tail towards longer wavelengths, see the profiles in Figure 5.1. In order to be able to detect the fluorescence spectra over a wide wavelength range the filter edge should be placed as close to the LED emission profile as possible, see Figure 5.4.

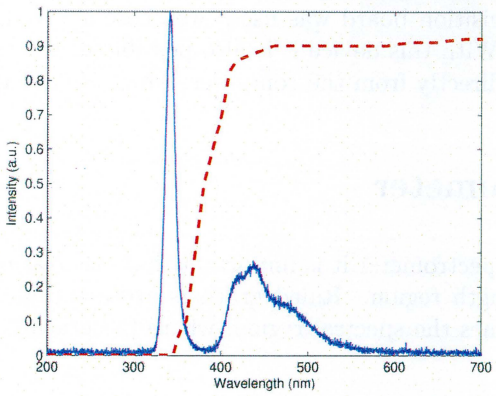

Figure 5.4: Fluorescence spectrum from a piece of white paper with excitation wavelength 340 nm; the red dotted line indicating where the filter GG385 will suppress the light.

If the profile is broad and the filter overlaps the profile slightly a strong background distribution of reflected light will be detected and could be mistaken for a fluorescence peak. If this is the case a bandpass filter could be placed in front of the LED. If the bandpass filter does not cover the whole intensity range it can be combined with a interference filter. Another possibility is to create an algorithm and mathematically suppress the reflection peak, since the shape of the reflection peak is known.

Care must be taken not to let the light pass too many filters. There is always a 4% reflection at every surface. The filter thickness hardly affects the losses in the system and it is often better to use a thick filter. With a thick filter the transmitted peak is hardly affected while the peaks in attenuated spectral regions are almost totally blocked. The relative intensity between two peaks is increased.

5.4.1 Rotating the filters

This fluorosensor accumulates several spectra using different excitation wavelengths. When the excitation wavelength is altered, the filter in front of the spectrometer needs to be altered simultaneously. This should preferably be done automatically, controlled via the computer used in the setup. Tunable electro-optic filters or liquid crystal filters would be perfect for the application since they change their cut-off wavelength when the applied electric field is changed. Unfortunately they are very expensive and not an option for this project. After careful consideration of different solutions a servo device was found to be the cheapest and smallest solution suitable for the application. It has a built-in

motor, gearbox, position feedback mechanism and controlling electronics. It is a small device that has an output shaft. This shaft can be positioned to specific angular positions by sending the servo control signals. The control pulse signal has a length of 1-2 ms and is repeated with the frequency 50 Hz. As long as the control signal is in the input line the servo will maintain the angular position of the shaft. When the pulse length changes, so does the position of the shaft [28].

In order to convert the digital signal from the computer to an analog control signal, a data acquisition board was used; we chose a DT 9812-10V National Instruments unit. With this device it is also possible to provide the servo with the power needed directly from the computer, which is desirable for field use.

5.5 Spectrometer

When choosing a spectrometer it is important that the grating is blazed to the interesting wavelength region. Ruled gratings are made with a certain blaze angle that determines the spectral region, where the grating has its maximum efficiency.

The entrance slit also influences the spectrometer resolution. A 100 μm entrance slit results in 5 nm resolution and a 200 μm entrance slit gives about 8 nm resolution in the particular spectrometer considered. For this application a 200 μm slit is the best choice because the LED emission profile, with 13 nm at FWHM, is still of crucial importance for the resolution. Using the larger entrance slit also allows more light into the spectrometer, and in that way the exposure time can be decreased which is of particular importance in the UV to avoid photobleaching of the sample. The integration time, or exposure time is set by the user in the software. It is equivalent to the shutter time on a camera: the amount of time the detector "looks" at the incoming photons.

The Ocean Optics USB4000 miniature fibre optic spectrometer used in the fluorosensor has a 3648 element linear CCD (Charge Coupled Device) array. A CCD array consist of densely packed Metal Oxide Semiconductors (MOS) on a semiconductor substrate (Si). MOSs are manufactured by oxidizing the substrate and attaching metal electrodes. The absorbed photons will be converted to charge carriers, the number of electrons created is proportional to the number of photons absorbed. If the substrate (Si) is p-doped a positive voltage on the electrode will cause the electrons to accumulate around it. Many electrons can be stored like this in every pixel; each pixel acts like a capacitor. If too many electrons are collected in one pixel, they may escape and be collected by a neighboring pixel. This phenomenon is called blooming, as mentioned in the section 5.3. The charges are shifted sidewise and will finally reach the output where they will be registered [25].

5.6 Software

To control the LEDs a digital signal is sent to the LED circuit board via the data acquisition board. The data acquisition board (daq), mentioned in section 5.4.1,

which converts the digital signal from the computer to a TTL-signal (Transistor-transistor logic), is easily connected to the computer via an USB. A high value turns the LED on and a low value shuts it off. The LED principal circuit board adjusts the current so that no more than 20 mA reach the diode, see Appendix A.2.

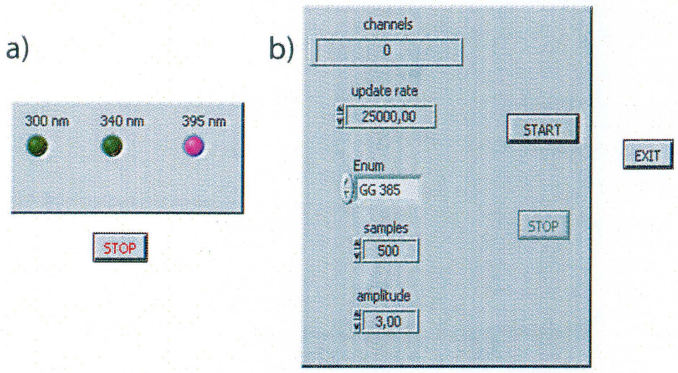

Figure 5.5: The front panels for controlling the LEDs (a) and the filters (b). All LEDs can independently of each other be switched on and off. The filter wheel is put into the correct position by choosing filter in the front panel.

To change the position of the filter wheel the servo needs a analog square signal at 50 Hz with a duty cycle between 1-2 ms as mentioned above. This is created in LabVIEW and generated in the acquisition board. The pulse duration determines the angular position of the shaft, see the software front panels in Figure 5.5.

The Ocean Optics program OOIBase32 is used to accumulate spectra. It has a user-friendly interface and allows the spectra to be easily saved.

Chapter 6

Measurements

6.1 Chlorophyll

Chlorophyll absorbs most strongly in the blue and red regions but poorly in the green, hence the green colour of chlorophyll-containing tissues like plant leaves. The LED 395 is the best one out of the three for absorption by the chlorophyll. In Figure 6.1 the fluorescence spectra from a green, a yellow and a brown leaf are shown for comparison. Chlorophyll absorbs so strongly that it can mask other pigment. Some of these pigments are revealed when the chlorophyll molecule decays in the autumn, the green colour fades and is replaced by red, yellow and golden brown. Apart from the change in colour this is also seen in the fluorescence signal since the fluorescence intensity is proportional to the fluorophore concentration. Also, the relative intensity of the two red peaks changes [29].

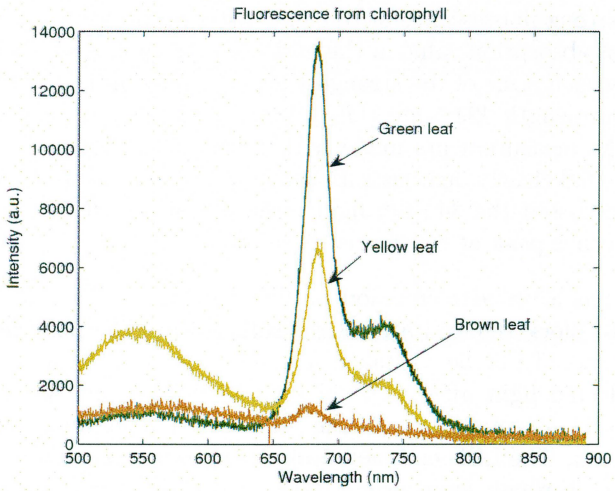

Figure 6.1: Fluorescence from a green, yellow and brown leaf, respectively. Excitation wavelength is 395 nm, integration time 7 seconds.

6.2 Europium-doped Yttrium Oxide

The fluorescence from a known phosphor, Europium-doped yttrium oxide ($Y_2O_3 : Eu^{3+}$) was measured. The temperature dependence of the fluorescence for this particular thermophosphor can be exploited for temperature measurement applications. All our measurements were performed in room temperature. When the yttrium oxide crystal matrix is doped with the Eu^{3+} ion, a broad absorption band occurs near 260 nm. This transition typically occurs when an electron is promoted from the oxygen to the europium ion. Essentially all fluorescence originates from this charge-transfer transition but also from the narrower absorption peaks due to atomic transitions. The excitation spectra for the 611 nm emission line, studied by Allison *et al.* [30] is presented in Figure 6.2.

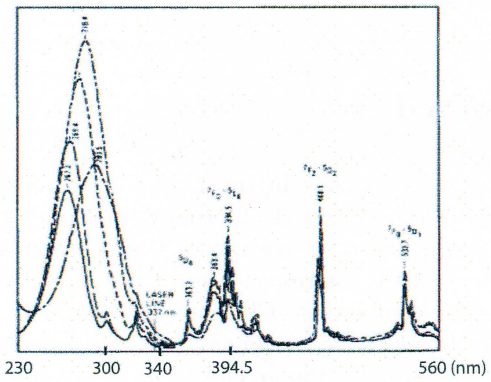

Figure 6.2: Excitation spectra ($Y_2O_3 : Eu^{3+}$) of emission as 611 nm for various temperatures. The solid line is at room temperature (From [30]).

The excitation wavelength 300 nm is within the europium absorption band and should induce strong fluorescence at 611 nm. 340 nm, on the other hand, possesses the lowest absorption value in the entire spectrum and will hardly stimulate any fluorescence. One of the strongest atomic emission transitions is found at excitation wavelength 394.5 nm ($^7F_2 - ^5L_6$), perfectly matched to the LED at 395 nm. The measurements made with the fluorosensor on $Y_2O_3 : Eu^{3+}$ shown in Figure 6.3 clearly demonstrate that the fluorescence is wavelength dependent. As discussed the 340 nm light is hardly absorbed by the phosphor, and the fluorescence peak at 611 nm is therefore missing.

The LED 395 has a broader emission profile, see Figure 5.1 and that is why the filter fails to block the excitation light sufficiently. The peak near 420 nm in Figure 6.3c should not be mistaken for fluorescence because it is reflected light. The reflected light affects the blue-green fluorescence so that it looks stronger than what it actually is. In the same manner the fluorescence affects the reflection peak. The LED emission profile is known and could be subtracted from the spectra through appropriate data processing, see section 8.3. The reason why the data in Figure 6.3a and b are noisier than c is that LED 395 generates a better signal; partially because that wavelength is well absorbed in the phosphor and partially because that diode has a higher output.

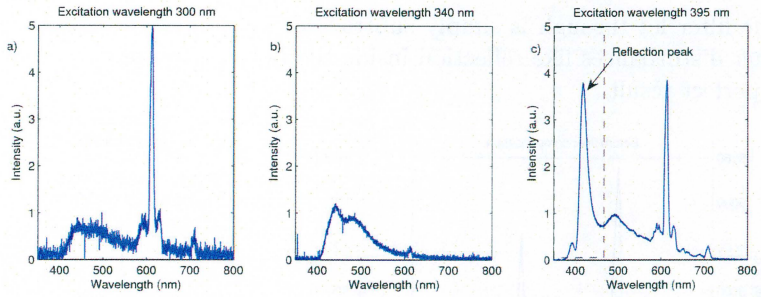

Figure 6.3: Emission spectra ($Y_2O_3 : Eu^{3+}$) after excitation by the three different LEDs: a) 300 nm, integration time 9 s. b) 340 nm, integration time 9s. c) 395 nm, integration time 4s. The peak to the left in c) is the reflection due to the filter fails to block the long-wavelength tail of the 395 nm excitation light.

6.3 Medical diagnosis of basal cell carcinoma

The usefulness of the fluorosensors in medical diagnostics was demonstrated at the Oncology clinic at the Lund University Hospital in diagnosing skin cancer. An ALA-containing cream had been applied on the patient tumours, located on the left side of the patient face, four hours before the planned treatment.

Before treatment the fluorescence from the patient tumour and area around the tumour was measured with the fluorosensor. The light output from the fibre probe is low, hence the sample needs to be illuminated for 15 seconds to collect sufficient fluorescence. After that the malignant area was illuminated with therapeutic light for about five minutes. The therapeutic light with the wavelength 633 nm is absorbed in the sensitizer and the energy is transferred to an oxygen molecule leading to destruction of the surrounding cancer cells. To validate the treatment efficiency the same measurement as before the treatment was performed with the fluorosensor for comparison. There should no longer be a PpIX signal, because of bleaching by the therapeutic light.

The following measurements were made with two different LEDs (395 nm and 340 nm):

- 10 mm to the left of the tumour border
- 5 mm to the left of the tumour border
- on the left border
- three measurements in the middle of the tumour
- on the right border
- 5 mm to the right of the tumour border
- 10 mm to the right of the tumour border

The spectra to the left of the tumour were averaged for each excitation wavelength, as were the measurements from the middle and on the right side. Because the filter does not block out the whole LED 395 emission profile (as discussed above) this was subtracted. That can be made in many ways; here the profile

that the filter let through is simply subtracted, see Figure 6.4. Because there are other disturbances like reflection inside the box the compensation does not give a perfect result.

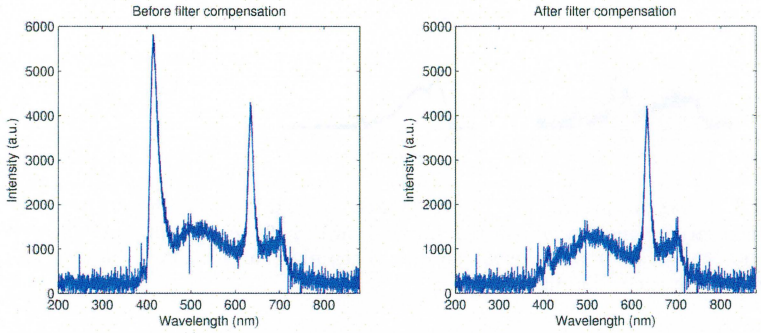

Figure 6.4: The PpIX fluorescence before and after compensation for the reflected light reaching the spectrometer.

Because of the considerable integration time the spectra were quite noisy, see Figure 6.4. To clarify the results the spectral data was processed. All spectra were smoothen out by averaging ten values to one along the intensity vector. The results are presented in Figure 6.5.

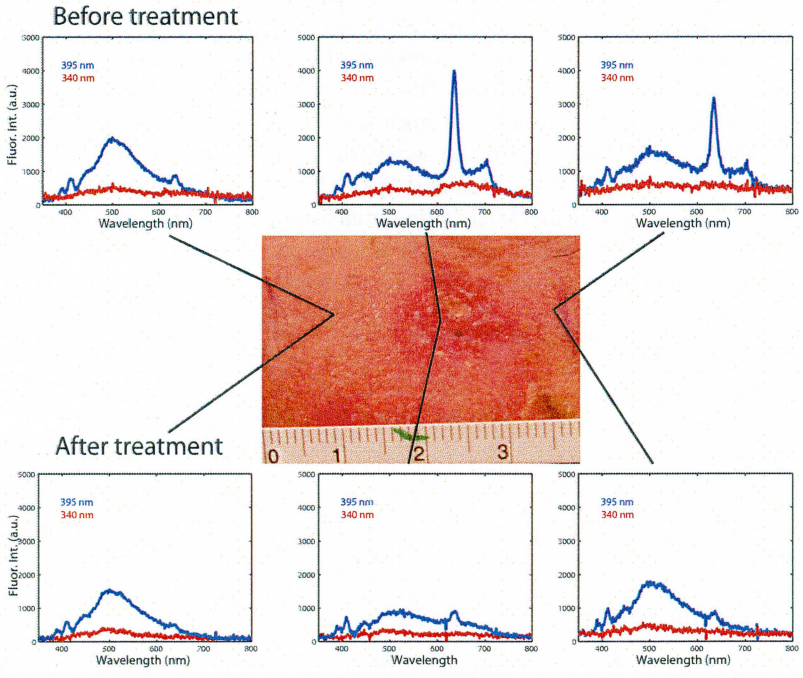

Figure 6.5: The fluorescence from a skin cancer tumour and the surrounding tissue. The excitation wavelengths 395 nm (the blue spectra) and 340 nm (the red spectra) are used.

The tumour tissue is characterized by a strong intensity increase at 635 nm due to the sensitizer, and a reduction of the skin autofluorescence. The area to the left, outside the tumour border show only a week signal at 635 nm. This

indicates that it is healthy skin with a normal autofluorescence. When the approaching the middle of the tumour from the border the intensity at 635 nm is increased, as expected. The spectra from outside the tumour on the right side show PpIX fluorescence even though the tissue looks healthy. The doctor confirms that the tumour is suspected to extend beyond the visible border. The treatment was successful, the 635 nm intensity peak is greatly reduced after the treatment, which imply that it has absorbed the therapeutic light. The tissue autofluorescence is still reduced in the tumour area. The sensitizer has a series of absorption bands in the visible spectrum, but not below the Soret band at 400 nm. As the Figure 6.5 shows the 340 nm excitation wavelength provide very little, if any, information because of its non matching energy.

To enhance the contrast in the spectra it can be processed further. The background can be reduced by subtracting the signal at 635 nm by the signal at about 600 nm, this intensity can be divided with the autofluorescence intensity, resulting in a dimensionless quantity with immunity to detection geometry etc [31].

Chapter 7

Summary and Conclusions

This Master's thesis has demonstrated that expensive lasers in present fluorosensors can be replaced with LEDs. The broad LED emission profile will excite molecules to different vibrational states, but because of the relaxation to the S_1 state they will all contribute to the emitted energy corresponding to the molecule band gap. The broad emission profile from an LED will therefore not affect the resolution of the fluorescence signal. The light output from an LED is high, it is the wide numerical aperture that causes problem. Even though only a fraction of the light was collected in the fibre it was sufficient to provide a clear fluorescence signal, making it possible to characterize the sample.

Several measurements were performed to prove the systems function. The fluorescence from a basel cell carcinoma was measured and showed good result and provided a correct medical diagnose. The tumours responds to treatment was clearly shown in the spectra. Because of the well-encapsuled optics and the special designed probe the system is well protected from surrounding light.

A lot of effort has been made to minimize the volume and it could not be made any smaller with the present equipment. It is designed for field use with the system self-sufficient of power (batteries inside the fluorosensor and the laptop computer provide the power needed). To enable a quick multi-wavelength measurements the system is fully computer controlled and the fluorosensor lid can remain closed.

Clearly, within the scope of this strictly time-limited project many aspects could only be given a first consideration. In the next section we discuss possible, desirable further developments.

Chapter 8

Future improvements

8.1 Signal enhancement

To get an idea of how much of the emitted light that actually illuminates the sample a relative measurement was performed. For that purpose a photodiode detector, pin-10DP/SB Edmund Optics, was used. First the induced voltage when the fibre was facing the diode was measured and after that the full LED radiation fell on the detector. Since the photodiode detector window is about 20 mm in diameter most of the LED light is thought to be detected. The result was that 0.2% of the LED output is coupled through the fibre. Expected value was about 3%, based on own calculations and the results from other researchers like Kawasaki, Johnson [32], Colvin [33]. Using ray tracing techniques the coupling efficiency has been estimated to approximately 10% for our situation and 15% with a bulb ended fibre (see Figure 8.1). The fact that a split fibre is used was thought to reduce the calculated value with about 70%. It seams like the coupling efficiency is even worse than expected, which in one way is encouraging; there is a lot of light to collect if the coupling is improved.

It is difficult to find UV LEDs with more output power than the ones used in this fluorosensor. An exception is the Cree XLAMP 7090 UVV with a radiant flux 200 mW, but it exists only in the wavelength range 390-410 nm. But the key to stronger signals is not only the power radiated by the source, but the power coupled into the optical fibre. Only a few percent of the emitted light is collected in the fibre. The coupling LED fibre needs to be optimized.

A lens that focuses the light into the fibre would probably help but was not tested in this project. The reason was that lenses which transmit UV are expensive and the ball lens shaped epoxy layer on the LEDs was thought to focus the light well. A reflector would probably also help focus more photons into the fibre. An off-axis parabola was tested but did not enhance the coupling efficiency. A reflector shaped like a tube leading the light between the source and fibre could be an alternative.

There are many others who have addressed this problem before. Burrus, Jr., at the Bell Telephone Laboratories, developed the so called Burrus SLED (Surface

Emitting LED) in 1971. The idea was to place the fibre as close to the active area as possible by inserting the multimode fibre directly on the semiconductor chip, see a sketch in Figure 8.1. Any of the coupling techniques in Figure 8.1 can be used to improve the coupling efficiency. There are two different lens techniques in the figure. The lens focuses the divergent light from the LED so that it matches the acceptance cone of the optical fibre. Instead of placing the fibre in front of the LED and try to find the optimal position the fibre can be glued onto the LED in a so called pigtailed arrangement.

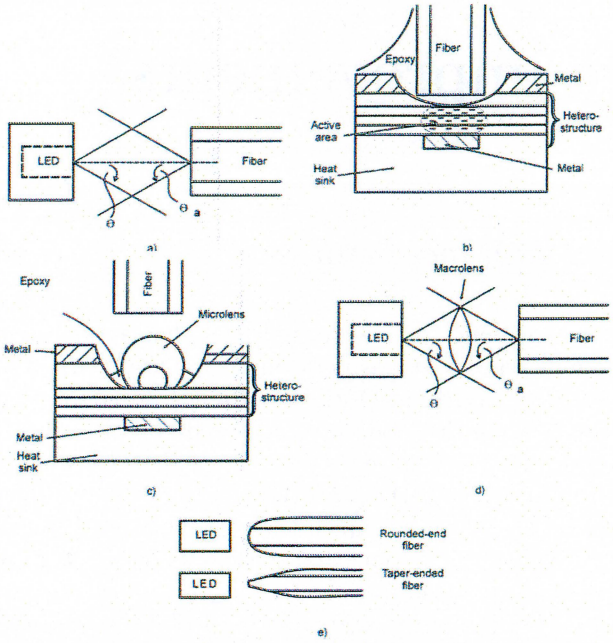

Figure 8.1: Coupling light from an LED into a fibre: a) The fibre facing the LED, used in this project b) Burrus SLED c) microlens coupling d) macrolens coupling e) rounded-end and tapered-end fibres (From [34]).

Another possibility is to glue a gradient-index (GRIN) lens onto a LED. A GRIN lens has a parabolic variation of refractive index. It focuses light like a conventional lens but does not need to be shaped like one. Bruno *et al.* [35] proposed this idea to improve the coupling efficiency. A hole was drilled in the plexiglas body of the LED, almost to the emitting crystal. A small GRIN lens was glued with UV-curing epoxy, see Figure 8.2. By arranging so that every component is in contact with each other the number of optical interfaces was reduced. Distances between elements are also reduced resulting in less optical losses. Another advantage is that everything is in one piece which means increased stability, less noise and less variation in component refractive indices.

Industrial Fibre Optics [37] produces fibre-optic LEDs utilizing the microlens coupling illustrated in Figure 8.1c. They have unfortunately only green LEDs but the idea is interesting. The LED is housed in a plastic fibre optic package with standard 1000 μm core plastic fibre-cable; see Figure 8.3.

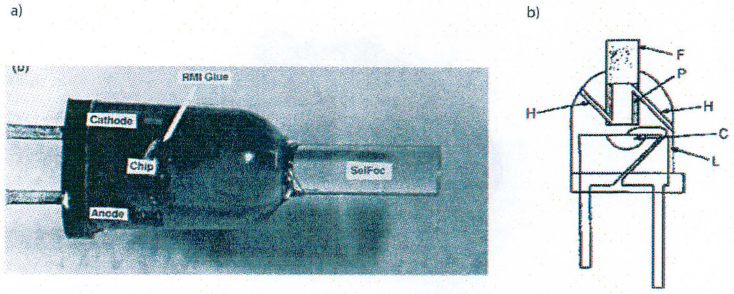

Figure 8.2: GRIN lens pigtailed to an LED. a) photograph. The cylindrical lens is visible inside the LED where it is fixated with refractive index matching glue. b) A schematic diagram. H: entrance/exit channels F: optical fibre P: opaque sleeve C: The semiconductor chip L: LED (From [36]).

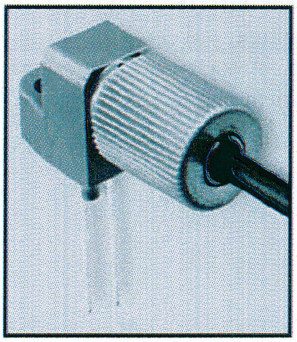

Figure 8.3: LED housed in a plastic fibre optic package (From [37]).

The optics on the detector side can also be optimized. A lot of light is lost in the lens coupling into the spectrometer. A well designed fibre port with possibilities to change filter or somehow placing the filters inside the spectrometer would be nice. The company m·u·t-gmbh sells an Inline Filter System; see Figure 8.4. The filter system has a female SMA connector on one side and a collimator with male SMA connector on the other end. It is easily coupled into the optical setup between the spectrometer and fibre. In this filter system there is no possibility to change filters, so it is not applicable in this project (but a reconstruction of the system would be interesting).

8.2 Software

The present software for the fluorosensor is far from perfect. It is enough to control the device and accumulate spectra but needs to be improved. The OMNIDRIVER from Ocean Optics was ordered for this project but has not been released yet. It is a universal driver for Windows that enables programming the spectrometer in LabVIEW. This is desirable since the LED-, filter-, and spectrometer control should be in the same programme. In the meanwhile an older version was delivered and hence the spectrometer programme OOIBase32

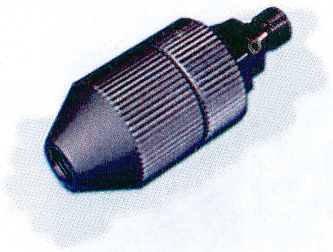

Figure 8.4: Inline Filter System from the company m·u·t-gmbh (From [38]).

was used in this project.

The ideal software has a user interface allowing use of non-specialists. The user begins with choosing which wavelengths to be used and then click on a "start measurement" button. After that the programme should repeatedly for all selected wavelengths perform the following tasks:

- Subtract background
- Put the correct filter into position
- Turn on the LED
- Accumulate spectrum
- Turn off the LED
- Process the spectra and present the result in a separate window.

8.3 Data analysis

When the LED emission profile is too wide so that the filter does not manage to cut off the excitation light completely, see Figure 6.3c, the reflection can be subtracted mathematically. An algorithm that suppresses the emission profile in every measurement would do the job. The LED emission profile is known; hence an algorithm that works satisfactory for every measurement can be constructed. If the LED emission profile could be measured and subtracted in the beginning of or continuously during the measurement, similar to the background subtraction the result would be better. To enable such a function a reference probe could be added to the fluorosensor construction. The probe could be a split fibre where three fibres becomes one leading light from each LED directly into the spectrometer. By continuously preforming this subtraction it will not matter if there are fluctuations in the excitation light. The easiest solution to the filter problem would of coarse be to find and purchase a LED 395 with a narrower emission profile.

A conventional fluorescence spectrum is either a plot over the luminescence intensity at a single excitation wavelength as a function of emission wavelength (an emission spectrum); see Figure 6.3, or a plot of the luminescence intensity

at a fixed emission wavelength as a function of excitation wavelength (excitation spectrum), see Figure 6.2. This fluorosensor has three different excitation wavelengths and a future device may have even more. In order to view all information in the same diagram the different spectra can be assembled into a fluorescence excitation-emission matrix (EEM). Then the fluorophore can be represented as a two dimensional matrix of fluorescence intensity as a function of both excitation and emission wavelength. The EEM helps to determine which excitation wavelengths that contain most diagnostic information [39].

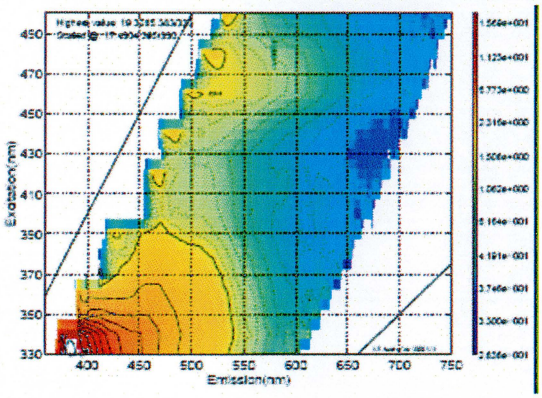

Figure 8.5: Typical example of an fluorescence EEM from a hamster cheek pouch (from [39]).

A further desirable feature would be to calibrate the system efficiency to provide a spectral correction using a calibrated Plack radiation source. This would lead to sharper signals in the UV and the deep red spectral regions where the system efficiency is lower.

Acknowledgements

First of all I would like to thank my supervisor Sune Svanberg. I appreciate his enthusiasm and ability to inspire others. All the discussions have been very educational and of crucial importance for this project. A special thanks to Benjamin Anderson, who was involved in the project before his return to Cape Coast, Ghana.

I am also very grateful to the following persons:

- Prof. Stig Bengmark for providing stimulus to the project regarding AGE.
- Mats Andersson for all his help with the software and electronics.
- Linda Persson for her positive attitude and for providing motivation and help.
- Rasmus Grönlund assisting in part of the data processing.
- Stefan Andersson-Engels for his valuable inputs on the project.
- Bertil Hermansson for constructing the LED driver and helping out with all engineering problems in the final construction. I appreciate his patience when I ran in and out of his office several times per day...

The fluorosensor would never be finished in time without the skillful employees at KI Maskinverkstad AB, who manufactured all the mechanical parts.

I would like to thank Katarina Svanberg and Niels Bendsoe for arranging for, and helping me with the clinical measurements.

Additionally, I would like to thank my fellow diploma students at the division, my family and friends for all support and encouragement.

A special thanks to the International Science Programme, Uppsala, represented by Lennart Hasselgren for promoting the cooperation with University of Cape Coast and providing financial support for a visit to Ghana, aiming at the testing of the fluorosensor in a realistic environment.

Bibliography

[1] U. Gustafsson, S. Pålsson, S. Svanberg: Compact Fiber-Optic Fluorosensor using a Continuous-Wave Violet Diode Laser and an Integrated Spectrometer. Review of scientific instruments **71**, 3004-3006 (2000)

[2] S. Svanberg: Laser Spectroscopy in Development. Europhysics News **33** 52-53 (2002)

[3] K. Svanberg, S. Svanberg: Bio-Medical Laser Physics in Development. Europhysics News **35**, No. 1 (2004)

[4] Wikimedia Foundation Inc: Light-Emitting Diode. http://en.wikipedia.org/wiki/Light_emitting_diode (2006-07-07)

[5] S. Wyckoff: What is a Light Emitting Diode? http://acept.la.asu.edu/courses/phs110/expmts/exp13a.html (2006-07-07)

[6] M. W. Davidson, M. Abramowitz, Olympus America Inc., and The Florida State University: Molecular expressions Microscopy Primer: Physics of Light and Color. http://micro.magnet.fsu.edu/primer/lightandcolor/ledsintro.html (2006-07-07)

[7] Wikipedia Foundation Inc: Laser Diode. http://en.wikipedia.org/wiki/Laser_diode (2006-07-12)

[8] S. Svanberg: Atomic and Molecular spectroscopy: Basic Aspects and Practical Applications, 4th ed. Springer-Verlag, Berlin Heidelberg New York (2003)

[9] J. R. Lakowicz: Principles of Fluorescence Spectroscopy. Plenum Press, New York (1983)

[10] Fluorescence Imaging with Medical Applications. Laboration instructions, Multispectral imaging (Atomic Physics Division, LTH)

[11] S. Bengmark: Advanced Glycation and Lipoxidation End products - Amplifiers of inflammation: The role of food. To be published.

[12] Wikimedia Foundation Inc: Advanced Glycation Endproduct. http://en.wikipedia.org/wiki/Advanced_glycation_endproduct (2006-08-14)

[13] G.N. Stamatas, R.B. Estanislao, M. Suero, Z.S. Rivera, J. Li, A. Khaiat, N. Kollias: Facial Skin Fluorescence as a Marker of the Skin's Response to Chronic Enviromental Insults and its Dependence on Age. Journal of Dermatology **154**, 125-132 (2005)

[14] R. Meerwaldt, R. Graaff, P.H.N. Oomen, T.P. Links, J.J. Jager, N.L. Alderson, S.R. Thorpe, J.W. Baynes, R.O.B. Gans, A.J. Smit: Simple Non-Invasive assessment of Advanced Glycation Endproduct Accumulation. Diabetologia **47**, 1324-1330 (2004)

[15] R. Na, I. M. Stender, H.C. Wulf: Can Autofluorescence Demarcate Basal Cell Carcinoma from normal Skin? A Comparison with Protoporphyrin IX Fluorescence. Acta. Derm. Venereol. **81**, 246-249 (2001).

[16] M. Panjehpour, C.E. Julius, M.N. Phan, T. Vo-Dinh, S. Overholt: Laser-Induced Fluorescence Spectroscopy for *in vivo* Diagnosis of Non-Melanoma Skin Cancers. Lasers in Surgery and Medicine **31**, 367-373 (2002)

[17] S. Pålsson: Methods, Instrumentation and Mechanisms for Optical Characterization of Tissue and Treatment of Malignant Tumours. PhD thesis, Lund, Sweden, 2003

[18] M. Soto Thompson: Photodynamic Therapy utilizing Interstitial Light Delivery Combined with Spectroscopy Methods. PhD thesis, Lund, Sweden, 2004.

[19] S.B. Brown: The Role of Light in the Treatment of Non-Melanoma Skin Cancer using Methyl Aminolevulinate. J. Dermatol. Treat. **14**, 11-14 (2003).

[20] J. Bublitz A. Christophersen W. Schade: Laser-Based Detection of PAHs and BTXE-aromatics in Oil Polluted Soil Samples. Fresenius J. Anal. Chem. **355**, 684-686 (1996)

[21] P. Weibring, H. Edner, S. Svanberg: Versatile Lidar System for Environmental Monitoring. Applied Optics **42**, 3583-3594 (2003)

[22] P. Juzenas, A. Juzeniene, O. Kaalhus, V. Iani and J. Moana: Non-invasive Fluorescence Excitation Spectroscopy during Application of 5-aminolevulinic Acid *in vivo*. http://www.rsc.org/publishing/journals /PP/article.asp?doi=b203459j (2006-11-15)

[23] Reflectivity Science - UV Coatings. http://www.optiforms.com/4000services/4100opticalCOATINGS/41404ocREFLECTIVITYuv.html (2006-10-20)

[24] J. Wallace: Deep-UV LEDs appear on the Market. Laser Focus World, http://lfw.pennnet.com/ (2006-08-12)

[25] S.G. Pettersson, S. Andersson-Engels, S. Kröll: Photonics and Optical Communication. Department of Physics, LTH (2005)

[26] The Nonimaging Optics Page, 3-D Profile of Refractive Secondary. http://hep.uchicago.edu/solar/NIoptics.html (2006-08-10)

[27] Optical Glass Filters made of Schott Filter Glass. Präzisions Glas & Optik http://www.pgo-online.com/intl/katalog/schott.html (2006-07-26)

[28] T. Engdahl: RC Servo Controlling. Last modification 2002-05-28 http://www.epanorama.net/documents/motor/rcservos.html (2006-08-01)

[29] B. Anderson, P. K. Buah-Bassuah J. P. Tetteh: Using Violet Laser-Induced Chlorophyll Fluorescence Emission Spectra for Crop Yield Assessment of Cowpea (*Vigna unguiculata (L) Walp*) varieties. Meas. Sci. Technol. **15**, 1255-1265 (2004)

[30] S.W. Allison, D.L. Beshears, M.R. Cates, A.R. Bugos: Emission Properties of Phosphors for High Temperature Sensor Applications. The University of Tennessee-Knoxville TN, Martin Marietta Energy Systems-Oak Ridge TN.

[31] S. Svanberg: Enviromental and Medical Applications of Photonic Interactions. Physica Scripta. **T110**, 39-50 (2004)

[32] B. S. Kawasaki, D. C. Johnson: Bulb-Ended Fibre Coupling to LED Sources. Optical and Quantum Electronics **7**, 281-288 (1975)

[33] J. Colvin: Coupling (launching) Efficiency for a Light-Emitting Diode, Optical Fibre Termination. Opto-Electronics **6**, 387-392 (1974)

[34] D. K. Mynbaev, L. L. Scheiner: Light Emitting diodes (LEDs). National instruments http://zone.ni.com/devzone/cda/ph/p/id/130 (2006-11-18)

[35] A. E. Bruno, F Maystre, B. Krattiger, P. Nussbaum, E. Gassmann: The Pigtailing Approach to Optical Detection in Capillary Electrophoresis. Trends Anal. Chem. **13**, 190-198 (1994)

[36] E. Verpoorte: Chip Vision-Optics for Microchips. The Royal Society of Chemistry 2003, 3, 42N-52N http://www.rsc.org/delivery/_ArticleLinKing/DisplayArticleForFree.cfm?doi=b307927a&JournalCodeLC (2006-11-18)

[37] Plastic Fiber Optic Green LED. http://www.i-fiberoptics.com/leds/IFE93.pdf (2006-11-18)

[38] Inline Filter System. http://www.mut-gmbh.de/en/products/optical_systems/elemente/20060307142419.html (2006-11-19)

[39] L. Coghlan, U. Utzinger, R. Drezek, D Heintzelman, A. Zuluaga, C. Brookner, R. Richards-Kortum, I Gimenez-Conti, M. Follen: Optimal Fluorescence Excitation Wavelengths for Detection of Squamous Intra-Epithelial Neoplasia: Results from an Animal Model. Optics Express **7**, 436 (2000)

Appendix A

Construction kit

A.1 Parts lists and budget

Item	*Price (EUR)*
USB4000 Plug-and-Play Miniature Fiber Optic Spectrometer	2804
OMNIDRIVER (for future use)	365
LED 300 nm UVTOP300-BL-TO39	260
LED 340 nm UVTOP340-BL-TO39	190
LED 395 nm LED395-02V	6
DT9812-10V Data Acquisition card	345
Filter WG320, GG385, GG420	220
Lens	100
Lensmount	150
Fibre	300
SMA connectors and fiber mounts	145
Servo	15
Box	20
Manufacturing (approx.)	1100
Total	6020

Quantity	*Product*	*Size (mm)*
2	screw	M5×50
3	screw	M5×20
8	screw	M5×15
4	screw	M5×10
3	screw	M5×8
2	screw	M4×12
1	screw	M4×10
2	screw	M3×10
15	screw	M3×5
13	nut	M5
6	nut	M4
11	nut	M3
9	washer	M5
9	washer	M4
2	washer	M3

A.2 The LED driver

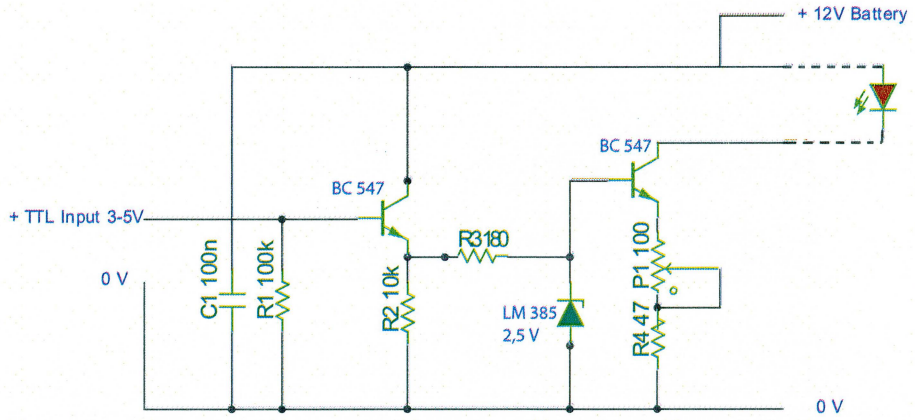

A.3 Drawings

Acquisition card mounting plate

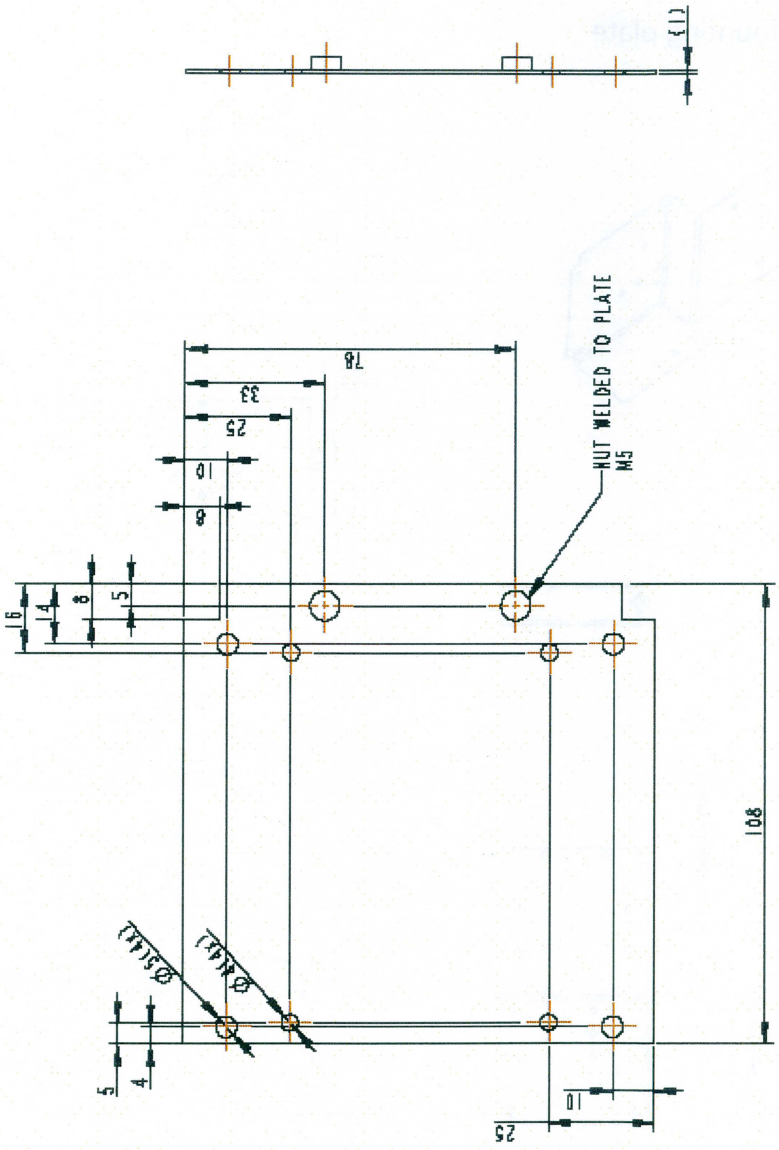

Mounting plate

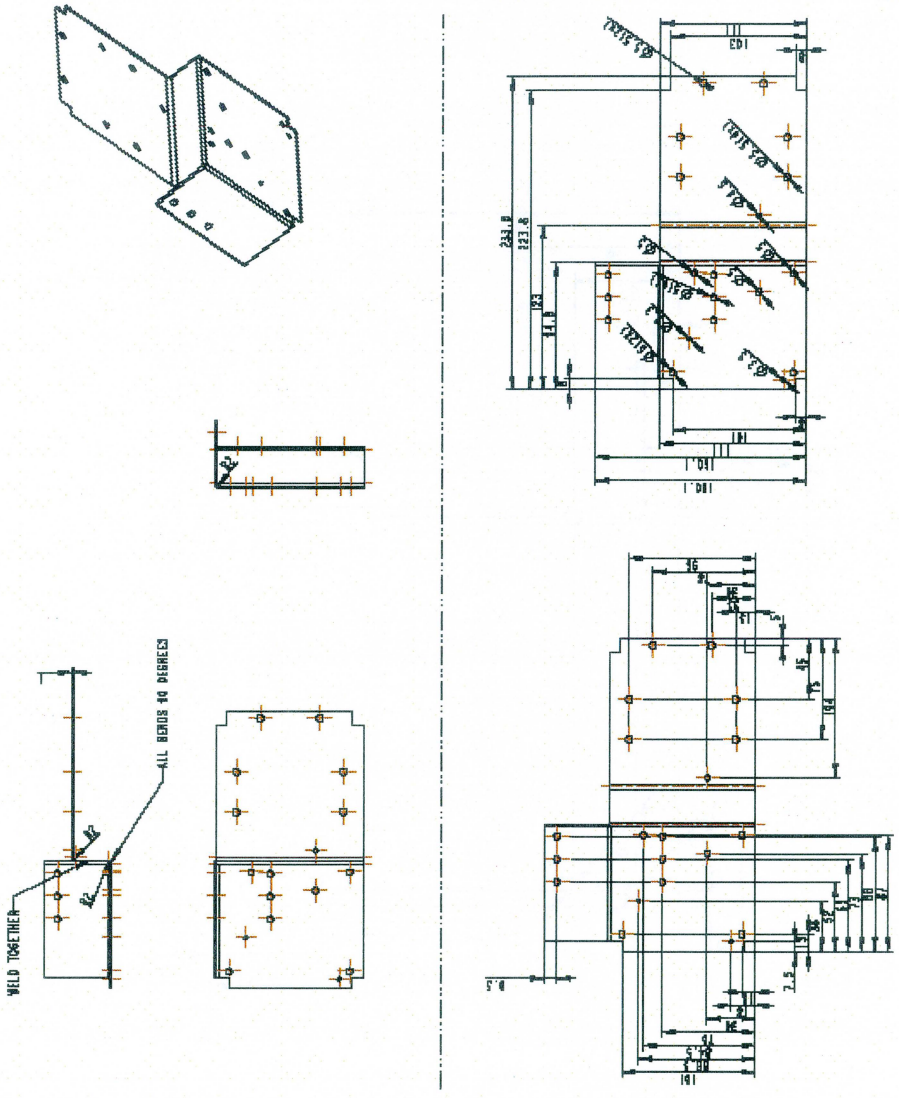

Servo mounting bracket

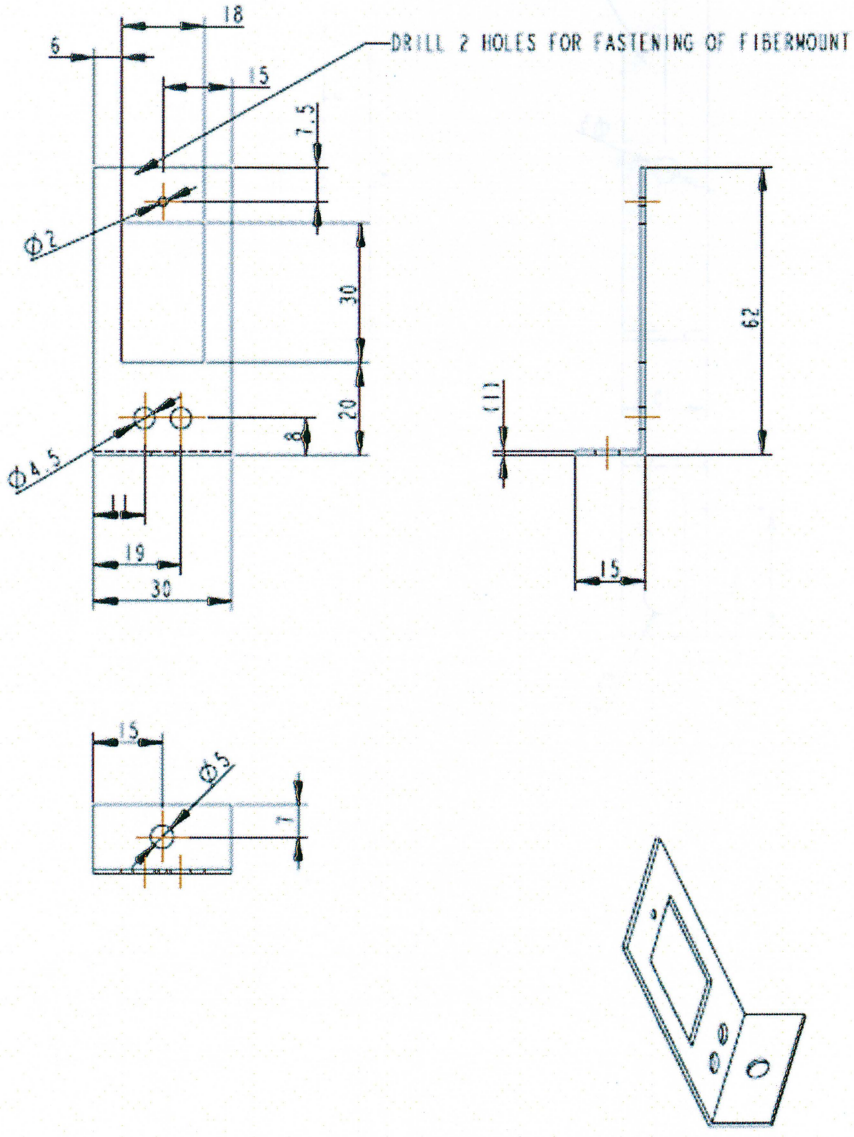

Fibre mounting bracket

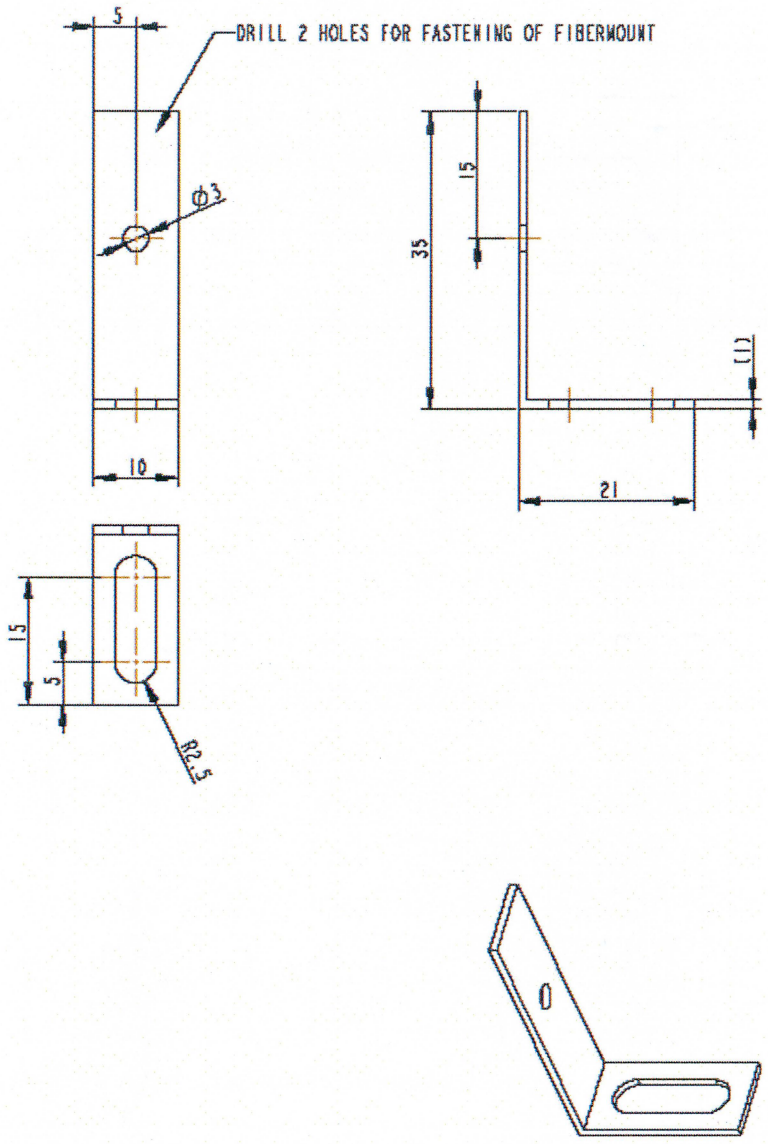

Spectrometer plates

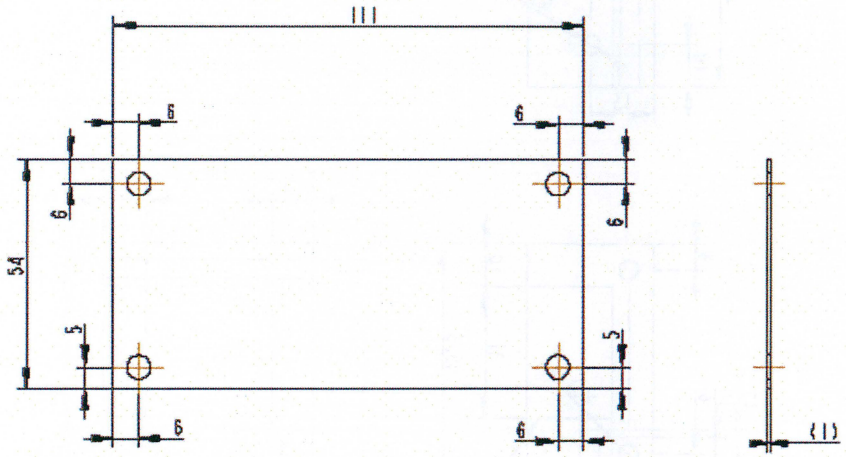

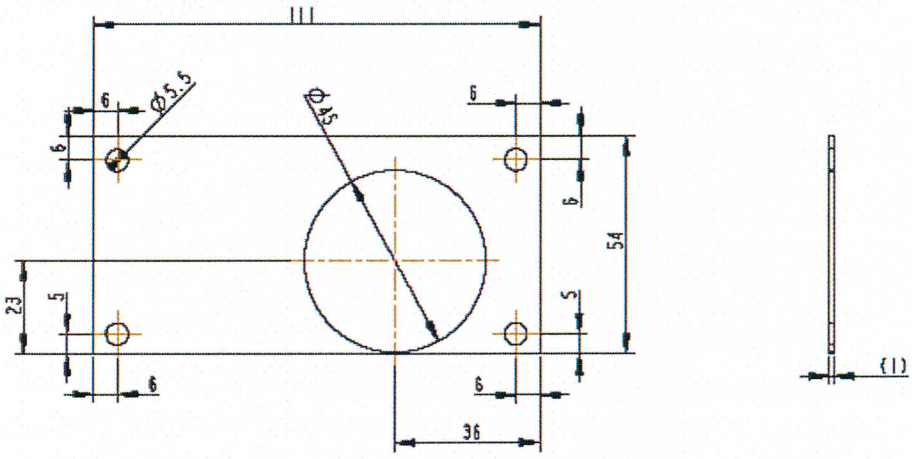

Spectrometer holder 1

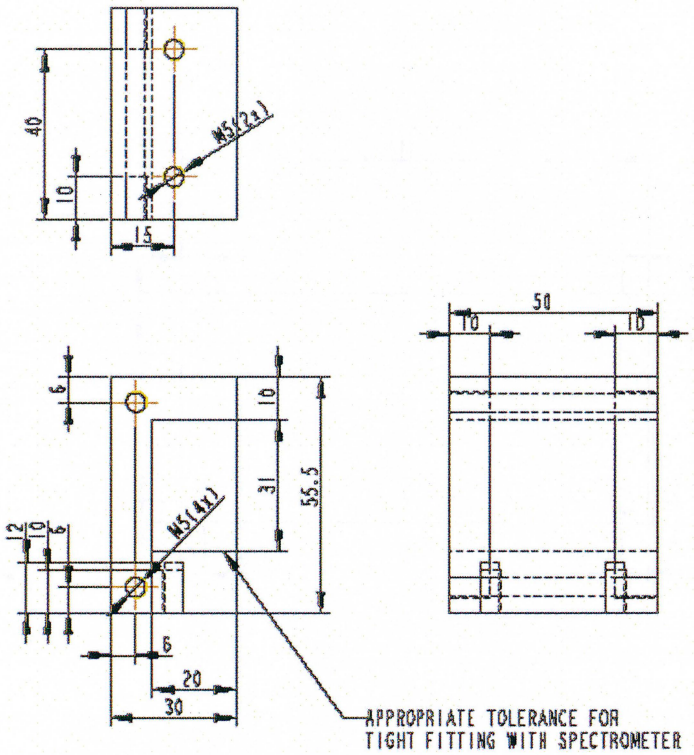

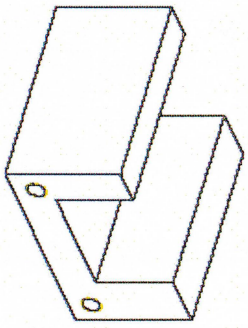

Spectrometer holder 2